Kinetic Analysis of a Molecular Model of the Budding Yeast Cell Cycle

Katherine C. Chen,* Attila Csikasz-Nagy,† Bela Gyorffy,† John Val,* Bela Novak,† and John J. Tyson*‡

*Department of Biology, Virginia Polytechnic Institute and State University, Blacksburg Virginia 24061; and †Department of Agricultural Chemical Technology, Technical University of Budapest, Gellert Ter 4, H-1521 Budapest, Hungary

The molecular machinery of cell cycle control is known in more detail for budding yeast, *Saccharomyces cerevisiae*, than for any other eukaryotic organism. In recent years, many elegant experiments on budding yeast have dissected the roles of cyclin molecules (Cln1–3 and Clb1–6) in coordinating the events of DNA synthesis, bud emergence, spindle formation, nuclear division, and cell separation. These experimental clues suggest a mechanism for the principal molecular interactions controlling cyclin synthesis and degradation. Using standard techniques of biochemical kinetics, we convert the mechanism into a set of differential equations, which describe the time courses of three major classes of cyclin-dependent kinase activities. Model in hand, we examine the molecular events controlling "Start" (the commitment step to a new round of chromosome replication, bud formation, and mitosis) and "Finish" (the transition from metaphase to anaphase, when sister chromatids are pulled apart and the bud separates from the mother cell) in wild-type cells and 50 mutants. The model accounts for many details of the physiology, biochemistry, and genetics of cell cycle control in budding yeast.

INTRODUCTION

To reproduce itself, a cell must duplicate all its components and separate them, more or less evenly, to two daughter cells, so that each daughter has the information and machinery necessary to repeat the process (Murray and Hunt, 1993; Alberts *et al.*, 1994, chap. 17). In general, eukaryotic cells replicate and partition their genetic material in two distinct, coordinated processes. During S phase, the DNA molecule in each chromosome is precisely replicated to form two identical sister chromatids that are held together by cohesins (tethering proteins). During M phase, the cell builds a mitotic spindle, condenses its replicated chromosomes, aligns them on the midplane of the spindle, and then, at anaphase, removes the cohesins and separates sister chromatids to opposite poles of the spindle (Biggins and Murray, 1998; Zachariae and Nasmyth, 1999). Shortly after anaphase, the cell divides into two daughter cells, each one containing a complete set of chromosomes. S and M phases are usually separated temporally by gaps (G1 and G2 phases).

It is crucial that each DNA molecule be replicated once and only once per cycle in eukaryotes. Were this not the case, then each chromosome would contain multiple sister chromatids, and segregation of the correct balance of DNA molecules to the spindle poles would be a difficult affair. This requirement is imposed by a set of proteins called licensing factors (Mcm2–7 and Cdc6). In the gap between the end of mitosis and the beginning of S phase, licensing factors bind to and prime the origins of replication. At the G1/S boundary, several cyclin-dependent protein kinases (CDKs) become active and initiate replication at licensed origins. In the process, the CDKs apparently incapacitate the license at each origin that fires. As long as CDKs remain active, throughout S, G2, and M, licensing factors remain incapacitated, and rereplication is impossible (Botchan, 1996; Wuarin and Nurse, 1996; Leatherwood, 1998).

It is also crucial that the cell does not commence anaphase (sister chromatid separation) until DNA replication is complete and each pair of sister chromatids is properly aligned on the metaphase plate. Completion of DNA synthesis is usually a requirement for entry into M phase, whereas chromosome alignment is required for activation of the anaphase-promoting complex (APC) that initiates degradation of an inhibitor of sister chromatid separation (Amon, 1999; Nasmyth, 1999). At anaphase, the APC also mediates proteolysis of mitotic cyclins, thereby destroying CDK activities and allowing licensing factors to accumulate and origins to be primed for replication.

‡ Corresponding author. E-mail address: tyson@vt.edu.
  Abbreviations: APC, anaphase-promoting complex; CDK, cyclin-dependent kinase.
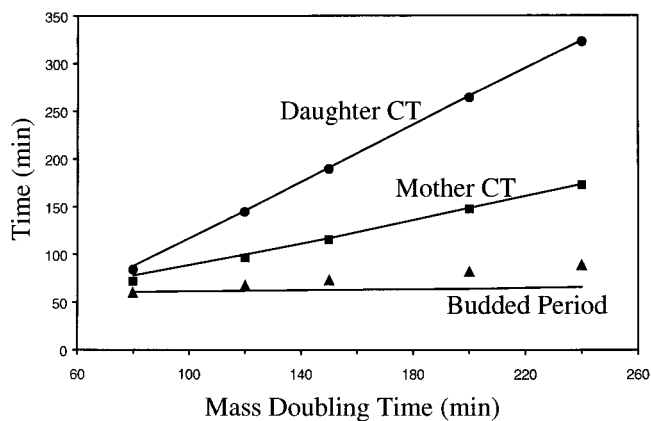
Figure 1. Mother and daughter cycle times (CT) as functions of the mass-doubling time of a culture. Lines, model simulations, calculated from the differential equations and parameter values in Tables 1 and 2. Symbols, experimental results from Lord and Wheals (1980): interdivision times of mothers (■) and daughters (●) and intervals from bud emergence to division (▲).

Third, the cell must coordinate its DNA replication–segregation cycle to cell growth, to maintain cell size within certain bounds, generation after generation. To achieve balanced growth and division, it is likely that some essential step in the cell cycle depends on the cell growing to a critical mass (Carter, 1981; Polymenis and Schmidt, 1999).

Although most eukaryotic cells satisfy these three requirements of DNA replication and division, there are notable exceptions, such as the cell cycles that produce oocytes, embryonic blastulas, and megakaryocytes. Furthermore, there are many variations in specific details from one cell type to another. For instance, budding yeast cells are peculiar in that they divide asymmetrically (Hartwell and Unger, 1977; Lord and Wheals, 1980). At Start, a bud emerges from the mother cell, and subsequent cytoplasmic growth is directed primarily to the bud. S and M phases are completed before the bud grows as large as its progenitor; thus cell separation produces a large mother cell and a small daughter cell. Shortly after division, the mother cell produces a new bud, but the daughter cell enters an extended G1 phase, during which it apparently must grow to a critical size before it can make a bud of its own. The whole process is quite sensitive to growth rate. At the fastest growth rates, division is almost symmetrical, and daughter cells have a short G1 phase as well. As growth rate is decreased, cell division becomes increasingly asymmetrical, and the G1 period of the daughter cell lengthens dramatically, whereas that of the mother cell remains relatively constant (Figure 1).

Another peculiarity of budding yeast is that cells progress simultaneously through S and M phases (DNA synthesis, spindle formation, and chromosome alignment), without any noticeable condensation of chromosomes. In this case, completion of DNA synthesis is not required for the early events of M phase but is required for the metaphase–anaphase transition (Nasmyth, 1995).

Nasmyth (1996) has proposed that the heart of the budding yeast cell cycle is an alternation between two self-maintaining states: the G1 state, in which APC is active,

CDK activity is low, and origins are licensed; and the S/M state, in which APC is shut off, CDK activity is high, and origins are fired and incapable of firing again. The G1 state is self-reinforcing because APC destroys S-phase and M-phase cyclins. The S/M state is self-reinforcing, suggested Nasmyth (1996), because CDKs inactivate the APC by phosphorylating some of its components. Although Nasmyth's proposal contradicted conventional wisdom that B-type cyclins activate the APC, recent experiments in budding yeast confirmed his hypothesis (Amon, 1997; Zachariae *et al.*, 1998; Jaspersen *et al.*, 1999). In Nasmyth's view, the budding yeast division cycle is an alternating sequence of "Start" transitions from G1 to S/M and "Finish" transitions from S/M back to G1. Our goals are to show how these two stable cell cycle states (G1 and S/M) arise from the underlying molecular machinery and to reveal the dynamical nature of the transitions (Start and Finish) between them.

To this end, we summarize experimental results from many sources to construct a consensus picture of the molecular signals controlling cell cycle events in budding yeast. The present picture is built on a simpler model of cell cycle controls in budding yeast (Tyson *et al.*, 1995) and on a mathematical description of Nasmyth's alternating-states hypothesis (Novak *et al.*, 1998). (Those models, along with earlier studies and reviews [Novak and Tyson, 1993, 1995, 1997; Tyson *et al.*, 1996, 1997], should be consulted for an introduction to our theoretical methods, strategies, and tools.)

After casting the mechanism into a set of kinetic equations, we study the dynamical properties of the control system by numerical simulations. Experimental data are used to estimate the crucial kinetic parameters in the model. Then the model is compared with the phenotypes of mutant cells in which various components of the control system are knocked out or overexpressed.

The model, which accounts for most of the distinctive characteristics of the budding yeast cell cycle, is valuable in bringing together a huge amount of hard-won experimental data in a convenient mathematical repository. As experimentalists think about yet unknown details around the "edges" of the consensus picture, the model can be used to explore the properties of hypothetical mechanisms. As new advances are made, the model can be extended to give an ever more comprehensive picture of cell cycle controls in budding yeast.

A CONSENSUS PICTURE OF CELL CYCLE CONTROLS IN BUDDING YEAST

Cyclin-dependent Kinase Activities

Major cell cycle events in budding yeast are controlled by a single CDK (Cdc28) in conjunction with two families of cyclins: Cln1–3 and Clb1–6 (Nasmyth, 1993; Mendenhall and Hodge, 1998). Cln1/Cdc28 and Cln2/Cdc28 play major roles in budding and spindle pole body duplication. Cln3/Cdc28 seems to govern the size at which newborn cells execute Start. Clb5/Cdc28 and Clb6/Cdc28 are essential for timely DNA replication. Clb3/Cdc28 and Clb4/Cdc28 seem to assist in DNA replication and spindle formation. Clb1/Cdc28 and Clb2/Cdc28 are necessary for proper completion of mitosis.

The roles of these cyclins overlap. All the single mutants are viable and nearly normal, except *cln3* mutants, which execute Start at about twice the size of wild-type cells (Dirick *et al.*, 1995). (Notation, for example, wild-type allele = *CLN3*, recessive mutant allele = *cln3*, dominant mutant allele = *CLN3*[D], and gene product = Cln3.) Although the *triple-cln* mutant, *cln1 cln2 cln3*, is lethal (Richardson *et al.*, 1989), the *cln1 cln2* double mutant is large and viable and able to bud. Apparently any one of the Clns can do the essential jobs of the other two, if the cell is large enough. The double mutant *clb3 clb4* is normal (Richardson *et al.*, 1992; Schwob and Nasmyth, 1993), so their roles can be played by other Clbs. Because a *clb5 clb6* mutant cell carries out DNA synthesis (although with some delay), whereas a cell with all six *CLB* genes deleted (*clb1–6*) does not, Clb1–4 can trigger DNA synthesis in the absence of Clb5–6 (Schwob *et al.*, 1994). Only the Clb1–2 pair is special in the sense that at least one of them is necessary for completing mitosis (Surana *et al.*, 1991). Because of these redundancies, it will be sufficient to consider the interaction of Cdc28 with only four classes of cyclins: "Cln2" (representing the combined activities of Cln1 and Cln2), Cln3, "Clb2" (Clb1 and Clb2 combined), and "Clb5" (Clb5 and Clb6 combined). We do not keep track of Clb3–4 in this model.

Regulation of Cyclin-dependent Kinase Activities

Cyclin/Cdc28 activities come and go in a characteristic sequence during the budding yeast cell cycle. Regulation is achieved mainly through the synthesis and degradation of cyclin components and of the Clb-dependent kinase inhibitor Sic1. Cln3 is present at low and nearly constant levels throughout the cell cycle; Cln2 and its associated kinase activity are maximal at Start (Wittenberg *et al.*, 1990; Tyers *et al.*, 1993). The pattern of Clb5 is similar to that of Cln2 (Schwob and Nasmyth, 1993), whereas Clb2 and its associated kinase activity peak ~10 min before anaphase (Surana *et al.*, 1991). Furthermore, Sic1 is present in high concentration in G1 and decreases to low levels after Start (Donovan *et al.*, 1994; Schwob *et al.*, 1994).

In many eukaryotic organisms, Cdk activity is also controlled by inhibitory phosphorylation at a conserved tyrosine in the N terminus of its kinase subunit. Although budding yeast has this tyrosine residue (Tyr-19 in Cdc28) and the kinase and phosphatase (Swe1 and Mih1) that regulate phosphorylation of this site, tyrosine phosphorylation does not play an important role in regulating Cdk activities during normal vegetative growth (Amon *et al.*, 1992; Sorger and Murray, 1992).

Transcription Factors

Expression of the *CLN2* gene (Koch *et al.*, 1996) is controlled by the transcription factor SBF (Swi4/Swi6) (Nasmyth and Dirick, 1991), which can be activated by all three Cln-associated as well as Clb5-associated kinases (Cross and Tinkelenberg, 1991; Schwob and Nasmyth, 1993) and inactivated by Clb2-associated kinase (Amon *et al.*, 1993). The transcription factor MBF (Mbp1/Swi6) for the *CLB5* gene is activated, like SBF, by the Cln- and Clb5-associated kinases (Koch *et al.*, 1993; Schwob and Nasmyth, 1993) but inactivated in G2 by some yet unknown mechanism other than Clb2/Cdc28 kinase (Amon *et al.*, 1993). Transcription of

CLB2 is autocatalytic, because Clb2/Cdc28 activates its own transcription factor (Mcm1/SFF) (Amon *et al.*, 1993; Maher *et al.*, 1995). Finally, *SIC1* transcription, regulated by Swi5, peaks at anaphase (Knapp *et al.*, 1996). Swi5 is inactivated by Clb2-dependent phosphorylation, which prevents it from entering the nucleus (Nasmyth *et al.*, 1990). It is activated, on the other hand, by a phosphatase, Cdc14, which is in turn activated indirectly by Cdc20 (Visintin *et al.*, 1998; Jaspersen *et al.*, 1999), an ancillary protein for the APC-dependent degradation machinery to be described in the next section.

Proteolysis

All cyclins are degraded by proteasomes, which destroy proteins that have been tagged by ubiquitin. Ubiquitin tagging is carried out by complex enzymatic machinery that activates ubiquitin molecules, recognizes appropriate proteins to be destroyed, and transfers activated ubiquitin to these doomed proteins (King *et al.*, 1996; Peters, 1998; Zachariae and Nasmyth, 1999). For cyclins, two ubiquitin-conjugating protein complexes are known: the APC and the SCF. The APC is composed of a dozen proteins, including Cdc16, -23, and -27, (Zachariae *et al.*, 1996). The SCF is a complex of Skp1, Cdc34, Cdc53, and an F box-containing protein, like Cdc4 or Grr1 (Jackson, 1996; Krek, 1998). The APC is responsible for destruction of Clb2 (Irniger *et al.*, 1995), Clb5 (partly) (Irniger and Nasmyth, 1997), Cdc20 (Shirayama *et al.*, 1998), and Pds1 (Yamamoto *et al.*, 1996), a protein that promotes sister chromatid cohesion until anaphase. The SCF is responsible for destruction of Cln2 (Deshaies *et al.*, 1995; Willems *et al.*, 1996), Cln3 (Yaglom *et al.*, 1995), and Sic1 (Feldman *et al.*, 1997). Because Clb5 is more stable in *skp1* mutants than in wild-type cells (Bai *et al.*, 1996), Clb5 may be partly degraded by SCF.

Both APC and SCF require ancillary proteins, whose job is to recognize appropriate protein substrates and present them to the ubiquitin-conjugating machinery. For example, Cdc4 presents Sic1, and Grr1 presents Cln2 and Cln3 to the SCF (Barral *et al.*, 1995; Feldman *et al.*, 1997; Li and Johnston, 1997; Skowyra *et al.*, 1997). In like manner, Hct1 (also called Cdh1) presents Clb2, and Cdc20 presents Pds1 and Clb5 to the APC (Schwab *et al.*, 1997; Visintin *et al.*, 1997).

The SCF seems to be active at all times in the cell cycle. Degradation of its target proteins is controlled by the phosphorylation state of the target (Willems *et al.*, 1996). For example, in G1 phase, Sic1 is unphosphorylated and stable, even though the SCF is active. When Cln2-associated kinase activity rises at Start, Sic1 is phosphorylated, and Sic1P is rapidly presented by Cdc4 to the SCF for ubiquitination and subsequent proteolysis (Verma *et al.*, 1997). Likewise, Cln2 must be phosphorylated before it is recognized by Grr1 (Barral *et al.*, 1995; Li and Johnston, 1997).

APC-dependent proteolysis, on the other hand, is controlled by phosphorylation of the ubiquitination machinery itself, rather than the target proteins. There is evidence in clam oocyte extract (Lahav-Baratz *et al.*, 1995; Sudakin *et al.*, 1995), *Xenopus* egg extract (Felix *et al.*, 1990; Peters *et al.*, 1996), and mammalian cells (Kotani *et al.*, 1998) that the APC core is activated by phosphorylation and that CDKs may be involved in this activation indirectly via a polo-like kinase (whose homologue in budding yeast is Cdc5) (Descombes and Nigg, 1998; Kotani *et al.*, 1998). But such effects are not

yet well established in budding yeast, so we do not try to model them in the present paper.

Rather, we focus on the ancillary proteins, which seem to exist in active and inactive forms. For the Hct1-dependent degradation machinery, Amon (1997) showed that, in vivo, cyclin proteolysis can be turned off by ectopic expression of Clb2 (and back on again by expression of Sic1). Recent experiments (Zachariae *et al.*, 1998; Jaspersen *et al.*, 1999) show that, in vitro, CDKs can phosphorylate Hct1, rendering it incapable of interaction with the APC core. Together, these findings confirm Nasmyth's (1996) hypothesis that CDK activity and Clb proteolysis are antagonistic events: CDK inactivates APC by phosphorylation, whereas APC destroys CDK activity by degradation of cyclin components. The phosphatase that opposes CDK (and thereby activates Hct1) is Cdc14. Notice that the kinase-phosphatase pair, CDK-Cdc14, regulates not only the activity of Hct1 but also the synthesis (Swi5) and degradation (phosphorylation state) of Sic1 (Visintin *et al.*, 1998; Jaspersen *et al.*, 1999).

The Cdc20-dependent degradation machinery is more complicated still. As cells exit from mitosis, it is responsible for degradation of Pds1, which restrains the dissociation of cohesins by binding to and inhibiting Esp1, a protein essential for sister chromatid separation (Ciosk *et al.*, 1998). Cdc20 is also responsible for loss of an inhibitor of Cdc14 (Novak *et al.*, 1999), leading to activation of Hct1 and Swi5 (Visintin *et al.*, 1997; Lim *et al.*, 1998; Shirayama *et al.*, 1998). The RENT complex, recently identified by Shou *et al.* (1999) and Visintin *et al.* (1999), may inhibit Cdc14 by reversible sequestration.

Mitotic Checkpoint

It has been shown (Hwang *et al.*, 1998) that Cdc20 is a likely target for signals from unaligned chromosomes, unreplicated DNA, and damaged DNA, all of which keep Cdc20 in its inactive form. Unreplicated DNA, in addition to keeping Cdc20 inactive, seems to impinge on the APC-activating pathway as well (Hwang *et al.*, 1998; Kotani *et al.*, 1998). The end result is that, when DNA replication is complete and all chromosomes are in tension on the metaphase plate, APC is phosphorylated, and Cdc20 is activated, leading to degradation of Pds1 (hence, dissolution of cohesions) and to activation of Hct1 (hence, destruction of Clb2).

KINETIC MODEL

From these facts we construct a consensus picture (Figure 2) of cell cycle controls in budding yeast. Using standard principles of biochemical kinetics, we cast the molecular mechanism into a set of nine, nonlinear, ordinary differential equations governing the temporal changes of cyclins and their regulatory proteins, plus four auxiliary differential equations describing cell growth and CDK-induced events (activation of DNA replication origins, bud emergence, and spindle assembly), plus three algebraic equations determining the activities of SBF, Mcm1, and Swi5 transcription factors (Table 1). About 50 parameters enter into the definitions of these equations, and their values (for wild-type cells) are specified in Table 2. Appendix A, describes how these parameter values were estimated.

The model involves a number of specific kinetic assumptions that are introduced either to simplify the model or to explain specific characteristics of wild-type and mutant cell cycles, as we shall describe. Here we list these assumptions for easy reference.

1) Cell size is coupled to the CDK engine by assuming that the synthesis of each cyclin is proportional to mass, a variable representing overall cell "size." (For simplicity, we assume that mass increases exponentially.) We have in mind that cyclins are synthesized in the cytoplasm, where ribosome number increases throughout the cycle, and accumulate in the nucleus, whose volume does not change much. Thus, the concentrations of cyclins in the nucleus, [Cln2], [Clb2], etc., tend to increase as mass increases. Although many experiments demonstrate that budding yeast division cycles are controlled by cell size (Carter, 1981) through effects on CDK activities (Baroni *et al.*, 1994; Tokiwa *et al.*, 1994; Polymenis and Schmidt, 1997), the molecular mechanism whereby cells measure their nucleocytoplasmic ratio has not yet been elucidated. Our hypothesis, although speculative, is the simplest way to couple growth and division.

2) Transcription of *CLB5* is controlled by MBF, but the signal that inactivates MBF is unknown at present, so our picture is incomplete. Because MBF and SBF turn on and off at similar times in the cell cycle, under most conditions (Koch and Nasmyth, 1994; Cho *et al.*, 1998; Spellman *et al.*, 1998), we assume for the time being that [MBF] = [SBF]. When MBF regulation is better understood, this part of the model can be easily improved.

3) The activation and inactivation of transcription factors (SBF, Mcm1, and Swi5) are modeled as Goldbeter–Koshland (1981) ultrasensitive switches, as described in Appendix B. We could have represented the sigmoidal behavior of these switches by simpler functions, but the Goldbeter–Koshland function is particularly suitable for the phosphorylation–dephosphorylation reactions typical of cell cycle controls.

4) Bck2 cooperates with Cln3 in activating SBF at Start.

5) At high dosage, the activity of Cln3-dependent kinase plateaus.

6) We assume first-order kinetics for degradation of Cln2 and Clb5 by SCF. We are aware that SCF-catalyzed ubiquitination depends on prior phosphorylation of its substrates, most likely by CDKs themselves. Nonetheless, we choose simple first-order kinetics for cyclin degradation in the present model. Later versions can be improved in this regard, if necessary.

7) To describe how CDK activities drive DNA synthesis, bud emergence, and mitotic events, we introduce three "target" variables: ORI, BUD, and SPN. These targets are phosphorylated by CDKs, and the associated physiological events occur when their cumulative level of phosphorylation reaches a threshold (1 in each case).

8) In the present model, Clb2-dependent kinase stimulates the synthesis of Cdc20 (Prinz *et al.*, 1998) and indirectly activates it by driving [SPN] toward 1. The function of [SPN] is to provide a time delay between the appearance of Clb2 and the activation of Cdc20. To model the effect of nocodazole, we block the activation of Cdc20.

9) Metaphase checkpoint controls are the most primitive part of the model. We assume that Cdc20 is kept inactive until all chromosomes are properly aligned on the mitotic spindle ([SPN] = 1). After it is activated, Cdc20 helps activate Hct1 and Swi5, presumably by degrading some inhibitor of Cdc14 (Novak *et al.*, 1999). In a later model, we will track the kinetics of Cdc14 and its sequestration in RENT complexes, but for now we simply allow Cdc20 to activate Hct1 and Swi5 directly.

10) Cdc20 degrades Clb2, to some extent.

Intuitively, the diagram in Figure 2 seems appealing, but the hand-waving arguments used to justify it are not entirely convincing. Exactly what experiments can this model account for and what does it leave unexplained? The only way to address this question is to study the mathematical model (Table 1) thoroughly and rigorously, comparing its solution with the physiology of real cells. Where there is a correspondence between the model and reality, we can have some confidence that our understanding of the budding yeast cell cycle is adequate. Where the model fails will point to aspects of the control system that need further study.

Figure 2. Molecular model of the control of CDK activities during the budding yeast cell cycle. We lump together redundant cyclins (Cln1 + Cln2 = "Cln2," Clb1 + Clb2 = "Clb2," and Clb5 + Clb6 = "Clb5") and ignore Clb3 and Clb4. (Notice that we do not draw the kinase subunit, Cdc28, that is associated with each cyclin, because we assume it is in excess.) At the beginning of the cycle, the cell has few cyclin molecules, because the transcription factors (SBF, MBF, and Mcm1) that regulate cyclin synthesis are inactive. Clb-dependent kinases, in addition, are suppressed by a stoichiometric inhibitor (Sic1) and by efficient proteolysis of cyclin subunits. Cln3/Cdc28, which is present at low and nearly constant activity throughout the cycle, triggers a sequence of events leading ultimately to cell division. The sequence can be read from left to right. When the cell grows to a sufficiently large size, Cln3/Cdc28 and Bck2 activate SBF and MBF (by phosphorylation, so we assume), causing Cln2 and Clb5 to begin to accumulate. At first, Clb5 accumulates in inactive trimers, Clb5/Cdc28/Sic1, but Cln2/Cdc28 is not so inhibited. Rising Cln2/Cdc28 activity plays three important roles.
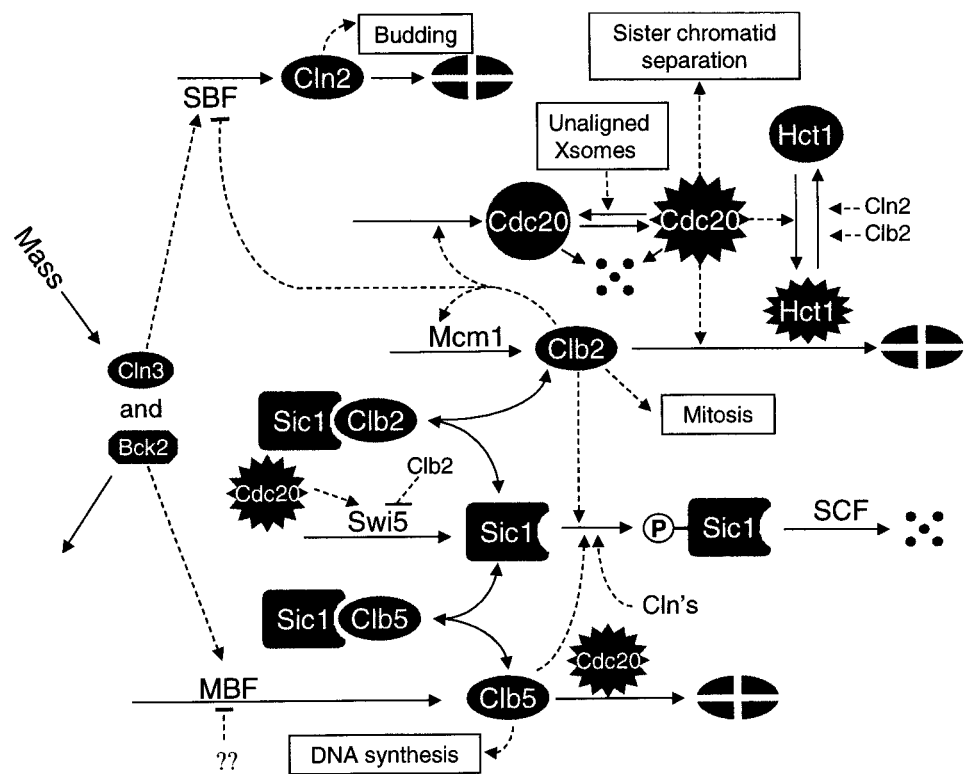
First, it initiates bud formation. Second, it phosphorylates Sic1, priming the inhibitor for ubiquitination by SCF and ultimate degradation by the proteasome. Third, it inactivates Hct1, which, in conjunction with APC, was responsible for Clb2 degradation in G1 phase. When Sic1 is destroyed, Clb5/Cdc28 activity rises abruptly and drives the cell into S phase. These are the major physiological events associated with the Start transition. With Sic1 gone and Hct1 inactivated, Clb2-dependent kinase can begin to rise, with some lag, because Clb2/Cdc28 activates its own transcription factor, Mcm1. In addition, Clb2/Cdc28 inactivates SBF, so Cln2-dependent kinase activity begins to fall as Cln2 synthesis shuts off. At about the same time, MBF is inactivated, and the Clb5 level starts to fall. Rising Clb2/Cdc28 activity induces progress through mitosis. The metaphase–anaphase transition is regulated by a pair of proteins, Cdc20 and Hct1, that target substrates to the APC for ubiquitination. At metaphase, they are inactive, but when DNA is fully replicated and all chromosomes are aligned on the metaphase plate, Cdc20 is activated. Indirectly Cdc20 promotes 1) dissociation of sister chromatids (anaphase A), 2) activation of Hct1, which conducts Clb2 to the APC, thereby initiating anaphase B and cell separation, and 3) activation of Swi5, the transcription factor for Sic1. With all CDK activity gone (except for a little associated with Cln3), Sic1 can make a comeback, and the cell returns to G1.

RESULTS

Wild-Type Cell Cycle

Figure 3 presents a numerical solution of the kinetic equations (Table 1), using a basal set of rate constants (Table 2), suitable for wild-type division cycles (see Appendix A for a justification of the parameter values). In this case, the mass-doubling time (T_d) of the culture is 120 min (specific growth rate = $\mu = 0.693/T_d = 0.005776$ min^{-1}). Because division is asymmetrical, we must distinguish between mother and daughter cells. The smaller daughter cells (Table 3, line 1) have a longer cycle time (146 min from birth to division), because they require more time to grow to the critical size when SBF turns on. (In our model, SBF is turned on abruptly by Cln3 when mass $\approx$ 1.1; see Appendix B.) Mother cells have a cycle time of 100 min, because they turn on SBF more quickly after division. On the other hand, the budded phases of mother and daughter cells are quite similar (~60 min).

Start and Finish. Two major transitions characterize wild-type cell cycles (Figure 3). At Start, a series of events is initiated in rapid succession: SBF turns on, Cln2 and Clb5 levels rise, Sic1 disappears, Hct1 turns off, and DNA synthesis and bud emergence commence. Shortly thereafter, Clb2 level rises and a spindle starts to form. At Finish, Cdc20 and Hct1 turn on, Clb2 is destroyed, and Sic1 makes a comeback. In simulations of various mutant strains, we will see how these chains of events can be dissociated.

The first event of Start is abrupt activation of SBF, when cells grow to a critical size, as demonstrated experimentally (Dirick *et al.*, 1995; Stuart and Wittenberg, 1995). In our simulations, SBF turns on abruptly because it is modeled as an ultrasensitive switch (Goldbeter and Koshland, 1981), driven by the accumulation of Cln3 and Bck2 in the nucleus as the cell grows to the critical size. When the combined activities of Cln3 and Bck2, $k_{a,sbf} \times \varepsilon_{sbf,n3} \times ([Cln3]^* + [Bck2])$, exceed the activity of the opposing phosphatase, $k_{i,sbf}$, then SBF turns on (see Appendix B). With our param-

---

Table 1. Mathematical model of the budding yeast cell cycle

	Notes

Equations governing cyclin-dependent kinases

$$\frac{d}{dt}[\text{Cln2}] = (k'_{s,n2} + k''_{s,n2}[\text{SBF}]) \cdot \text{mass} - k_{d,n2}[\text{Cln2}]$$

$$\frac{d}{dt}[\text{Clb2}]_T = (k'_{s,b2} + k''_{s,b2}[\text{Mcm1}]) \cdot \text{mass} - V_{d,b2}[\text{Clb2}]_T, \quad V_{d,b2} = k'_{d,b2}([\text{Hct1}]_T - [\text{Hct1}]) + k''_{d,b2}[\text{Hct1}] + k'''_{d,b2}[\text{Cdc20}]$$

$$\frac{d}{dt}[\text{Clb5}]_T = (k'_{s,b5} + k''_{s,b5}[\text{MBF}]) \cdot \text{mass} - V_{d,b5} \cdot [\text{Clb5}]_T, \quad V_{d,b5} = k'_{d,b5} + k''_{d,b5}[\text{Cdc20}]$$

$$[\text{Bck2}] = [\text{Bck2}]^0 \cdot \text{mass}, \qquad [\text{Cln3}]^* = [\text{Cln3}]_{max}\frac{D_{n3} \cdot \text{mass}}{J_{n3} + D_{n3} \cdot \text{mass}}$$

$$[\text{Clb2}]_T = [\text{Clb2}] + [\text{Clb2/Sic1}], \quad [\text{Clb5}]_T = [\text{Clb5}] + [\text{Clb5/Sic1}]$$

$$[\text{Sic1}]_T = [\text{Sic1}] + [\text{Clb2/Sic1}] + [\text{Clb5/Sic1}]$$

a

Equations governing the inhibitor of Clb-dependent kinases

$$\frac{d}{dt}[\text{Sic1}]_T = k'_{s,c1} + k''_{s,c1}[\text{Swi5}] - \left(k_{d1,c1} + \frac{V_{d2,c1}}{J_{d2,c1} + [\text{Sic1}]_T}\right) \cdot [\text{Sic1}]_T$$

$$\frac{d}{dt}[\text{Clb2/Sic1}] = k_{as,b2}[\text{Clb2}] \cdot [\text{Sic1}] - \left(k_{di,b2} + V_{d,b2} + k_{d1,c1} + \frac{V_{d2,c1}}{J_{d2,c1} + [\text{Sic1}]_T}\right) \cdot [\text{Clb2/Sic1}]$$

$$\frac{d}{dt}[\text{Clb5/Sic1}] = k_{as,b5}[\text{Clb5}] \cdot [\text{Sic1}] - \left(k_{di,b5} + V_{d,b5} + k_{d1,c1} + \frac{V_{d2,c1}}{J_{d2,c1} + [\text{Sic1}]_T}\right) \cdot [\text{Clb5/Sic1}]$$

$$V_{d2,c1} = k_{d2,c1}(\varepsilon_{c1,n3}[\text{Cln3}]^* + \varepsilon_{c1,k2}[\text{Bck2}] + [\text{Cln2}] + \varepsilon_{c1,b5}[\text{Clb5}] + \varepsilon_{c1,b2}[\text{Clb2}])$$

b

Equations governing the Clb degradation machinery

$$\frac{d}{dt}[\text{Cdc20}]_T = (k'_{s,20} + k''_{s,20}[\text{Clb2}]) - k_{d,20}[\text{Cdc20}]_T$$

$$\frac{d}{dt}[\text{Cdc20}] = k_{a,20}([\text{Cdc20}]_T - [\text{Cdc20}]) - (V_{i,20} + k_{d,20}) \cdot [\text{Cdc20}]$$

$$V_{i,20} = \begin{cases} k'_{i,20}, & \text{for END\_M + 12 min} < t < \text{START\_S} \\ k''_{i,20}, & \text{for START\_S} < t < \text{END\_M} \end{cases}$$

$$\frac{d}{dt}[\text{Hct1}] = \frac{(k'_{a,t1} + k''_{a,t1}[\text{Cdc20}]) \cdot ([\text{Hct1}]_T - [\text{Hct1}])}{J_{a,t1} + [\text{Hct1}]_T - [\text{Hct1}]} - \frac{V_{i,t1}[\text{Hct1}]}{J_{i,t1} + [\text{Hct1}]}$$

$$V_{i,t1} = k'_{i,t1} + k''_{i,t1}([\text{Cln3}]^* + \varepsilon_{i,t1,n2}[\text{Cln2}] + \varepsilon_{i,t1,b5}[\text{Clb5}] + \varepsilon_{i,t1,b2}[\text{Clb2}])$$

c

Equations for growth, DNA synthesis, budding and spindle formation

$$\frac{d}{dt}\text{mass} = \mu \cdot \text{mass}, \quad \frac{d}{dt}[\text{ORI}] = k_{s,ori}([\text{Clb5}] + \varepsilon_{ori,b2}[\text{Clb2}]) - k_{d,ori}[\text{ORI}]$$

$$\frac{d}{dt}[\text{BUD}] = k_{s,bud}([\text{Cln2}] + [\text{Cln3}]^* + \varepsilon_{bud,b5}[\text{Clb5}]) - k_{d,bud}[\text{BUD}], \quad \frac{d}{dt}[\text{SPN}] = k_{s,spn}\frac{[\text{Clb2}]}{J_{spn} + [\text{Clb2}]} - k_{d,spn}[\text{SPN}]$$

d

Equations governing transcription factors

$$[\text{SBF}] = [\text{MBF}] = G(V_{a,sbf}, k'_{i,sbf} + k''_{i,sbf}[\text{Clb2}], J_{a,sbf}, J_{i,sbf}), \quad V_{a,sbf} = k_{a,sbf}([\text{Cln2}] + \varepsilon_{sbf,n3}([\text{Cln3}]^* + [\text{Bck2}]) + \varepsilon_{sbf,b5}[\text{Clb5}])$$

$$[\text{Mcm1}] = G(k_{a,mcm}[\text{Clb2}], k_{i,mcm}, J_{a,mcm}, J_{i,mcm}), \quad [\text{Swi5}] = G(k_{a,swi}[\text{Cdc20}], k'_{i,swi} + k''_{i,swi}[\text{Clb2}], J_{a,swi}, J_{i,swi})$$

e

Symbols, V = rate functions, k = rate constant, J = Michaelis constant. Subscripts, s = synthesis, d = degradation, a = activation, i = inactivation, as = association, di = dissociation, T = total.

[a] $k'_{d,b5}$ refers to SCF-mediated degradation of Clb5, and $k''_{d,b5}$ refers to its APC-mediated degradation.

[b] d1,c1 refers to the degradation of unphosphorylated Sic1. d2,c1 refers to the rate of phosphorylation of Sic1 by cyclin-dependent kinases, assuming that phosphorylated Sic1 is rapidly proteolyzed, releasing active Cdc28/Clb dimers.

[c] START_S is the time when [ORI] = 1, and END_M when [SPN] = 1. For START_S < t < END_M, there is a strong inhibitory signal on Cdc20 ($V_{i,20}$ = 10). Once the cell reaches metaphase (t = END_M), $V_{i,20}$ drops linearly from 10 to 0.1 over 12 min. Thereafter, $V_{i,20}$ = 0.1 until the start of the next S phase.

[d] Cell division occurs, we assume, when [Clb2] drops below a threshold (0.3). At this time, we divide mass between mother and daughter cells as follows: (mass of daughter cell at birth) = $f \times$ (mass at cell separation), (mass of mother cell at birth) = $(1 - f) \times$ (mass at cell separation), with $f = e^{-\mu D}$, where $D = (1.026/\mu) - 32$ is the observed daughter cell cycle time (Lord and Wheals, 1980). (See text for a discussion of the rule for asymmetric division.) At division, we also reset BUD and SPN to zero; however, we reset ORI to zero (for licensing factor to reappear after mitosis) only when [Clb2] + [Clb5] drop below a different threshold (0.2).

[e] $G(V_a, V_i, J_a, J_i)$ is the Goldbeter–Koshland function described in Appendix B.

eter values, Cln3 and Bck2 contribute about equally to the activation of SBF.

Finish (exit from mitosis) is triggered by activation of Cdc20. After cells pass Start and begin to synthesize Clb2, Cdc20 accumulates at an increasing rate. But it remains inactive because of inhibitory signals from unreplicated DNA and unaligned chromosomes. When those events are completed and the inhibitory signals disappear, Cdc20 is

Table 2. Kinetic constants for the budding yeast model

Rate constants (min^{-1})

$k'_{s,n2} = 0$	$k''_{s,n2} = 0.05$	$k_{d,n2} = 0.1$	
$k'_{s,b2} = 0.002$	$k''_{s,b2} = 0.05$		
$k'_{d,b2} = 0.01$	$k''_{d,b2} = 2$	$k'''_{d,b2} = 0.05$	
$k'_{s,b5} = 0.006$	$k''_{s,b5} = 0.02$	$k'_{d,b5} = 0.1$	$k''_{d,b5} = 0.25$
$k'_{s,c1} = 0.02$	$k''_{s,c1} = 0.1$	$k_{d1,c1} = 0.01$	$k_{d2,c1} = 0.3$
$k_{as,b2} = k_{as,b5} = 50$	$k_{di,b2} = k_{di,b5} = 0.05$		
$k'_{s,20} = 0.005$	$k''_{s,20} = 0.06$	$k_{d,20} = 0.08$	
$k_{a,20} = 1$	$k'_{i,20} = 0.1$	$k''_{i,20} = 10$	
$k'_{a,t1} = 0.04$	$k''_{a,t1} = 2$	$k'_{i,t1} = 0$	$k''_{i,t1} = 0.64$
$k_{s,ori} = 2$	$k_{s,bud} = 0.3$	$k_{s,spn} = 0.08$	
$k_{d,ori} = k_{d,bud} = k_{d,spn} = 0.06$		$k_{a,sbf} = k_{a,mcm} = k_{a,swi} = 1$	
$k'_{i,sbf} = 0.5$	$k'_{i,sbf} = 6$	$k'_{i,swi} = 0.3$	$k''_{i,swi} = 0.2$
$k_{i,mcm} = 0.15$	$\mu = 0.005776$		

Characteristic concentrations (dimensionless)

$[Cln3]_{max} = 0.02$	$[Bck2]^0 = 0.0027$	$[Hct1]_T = 1$	
$J_{spn} = 0.2$	$J_{d2,c1} = 0.05$		
$J_{a,sbf} = J_{i,sbf} = 0.01$	$J_{a,mcm} = J_{i,mcm} = 1$	$J_{a,swi} = J_{i,swi} = 0.1$	$J_{a,t1} = J_{i,t1} = 0.05$

Kinase efficiencies (dimensionless)

$\varepsilon_{c1,n3} = 20$	$\varepsilon_{c1,k2} = 2$	$\varepsilon_{c1,b2} = 0.067$	$\varepsilon_{c1,b5} = 1$
$\varepsilon_{i,t1,n2} = 1$	$\varepsilon_{i,t1,b2} = 1$	$\varepsilon_{i,t1,b5} = 0.5$	
$\varepsilon_{ori,b2} = 0.4$	$\varepsilon_{bud,b5} = 1$	$\varepsilon_{sbf,n3} = 75$	$\varepsilon_{sbf,b5} = 0.5$

Other parameters (dimensionless)

$f = 0.433$	$J_{n3} = 6$	$D_{n3} = 1$

activated. Active Cdc20 turns on Hct1 by overwhelming the inhibition exerted on Hct1 by Clb2 (presumably by degrading some inhibitor of Cdc14). When Hct1 turns on, Clb2 is degraded, and the control system switches to the G1 state, in which the enemies of Clbs (Hct1 and Sic1) are active.

Response to α-Factor. When an asynchronous population of budding yeast cells is exposed to α-factor (mating pheromone), pre-Start cells are blocked in G1, but post-Start cells finish DNA replication, divide, and stop in the next G1 phase. α-factor initiates a signal transduction pathway that ultimately eliminates all Cln-dependent kinase activities (Chang and Herskowitz, 1990; Peter and Herskowitz, 1994; Wittenberg and Reed, 1996). To simulate α-factor treatment, we set the catalytic efficiencies of Cln2- and Cln3-dependent kinases to zero, 10 min after the time of α-factor addition (i.e., assuming a 10-min delay for signal transduction). We found a point of no return shortly before the onset of S phase.

Dependence of Cell Cycle Time on Growth Rate and Birth Size. Figure 1 shows how certain characteristics of wild-type cell cycles depend on mass-doubling time, as reported by Lord and Wheals (1980) and Hartwell and Unger (1977). As T_d increases (specific growth rate, μ, decreases), cell division becomes increasingly asymmetrical, daughter size at birth decreases, and the duration of its unbudded phase increases. The unbudded phase of mother cells also increases slightly with T_d.

To fit the model to these data, we must adopt a rule for partitioning cell size to mother and daughter at cell separation. The simplest rule ("Rule 1") would be to give to the daughter cell all growth from bud emergence to cell division and let mother retain the mass it had when the bud emerged. However, in this case, the mother would be able to

bud soon after its birth; hence it should not have an appreciable unbudded period, which is in contradiction to the observations of Lord and Wheals (1980) and Hartwell and Unger (1977). For the mother cell to have an unbudded period, its birth size must be smaller than the critical size for bud emergence. Furthermore, the calculated daughter cycle times at various growth rates are longer than the observed values. Both results reflect that Rule 1 is inadequate, it gives too much mass to mothers and too little to daughters.

Therefore, we adopt a different rule (Rule 2). Let f = fraction of mass given to the daughter at cell division ($0 < f \leq \frac{1}{2}$), and choose f to give the observed daughter cycle time (D) at any particular growth rate ($\mu = 0.693/T_d$). From our assumption that cells grow exponentially, (mother size at division) = (daughter size at birth) $\times e^{\mu D}$, so f = (daughter size at birth)/(mother size at division) = $e^{-\mu D}$. By using the empirical formula for daughter cycle time, D = $1.48 T_d - 32$ (Lord and Wheals, 1980, their Table 2) to calculate f, we ensure that the model fits the data for D as a function of T_d (Figure 1, top line).

Furthermore, (mother size at division) = (mother size at birth) $\times e^{\mu P}$, where P = mother cycle time, and (mother size at division) = (mother size at birth) + (daughter size at birth). Therefore, $1 = e^{-\mu P} + e^{-\mu D}$. This relation was originally derived by Hartwell and Unger (1977) in a more complicated manner and shown by them to be consistent with the data. Consequently, by choosing f to fit D as a function of T_d, we also ensure a good fit to P as a function of T_d (Figure 1, middle line).

The dependence of budded period on growth rate (Figure 1, bottom line) is unconstrained, so its fit to the data is a valid test of the model. Progression through the budded part of the cycle is slightly dependent on growth rate but not nearly so much in the model as in experiments.
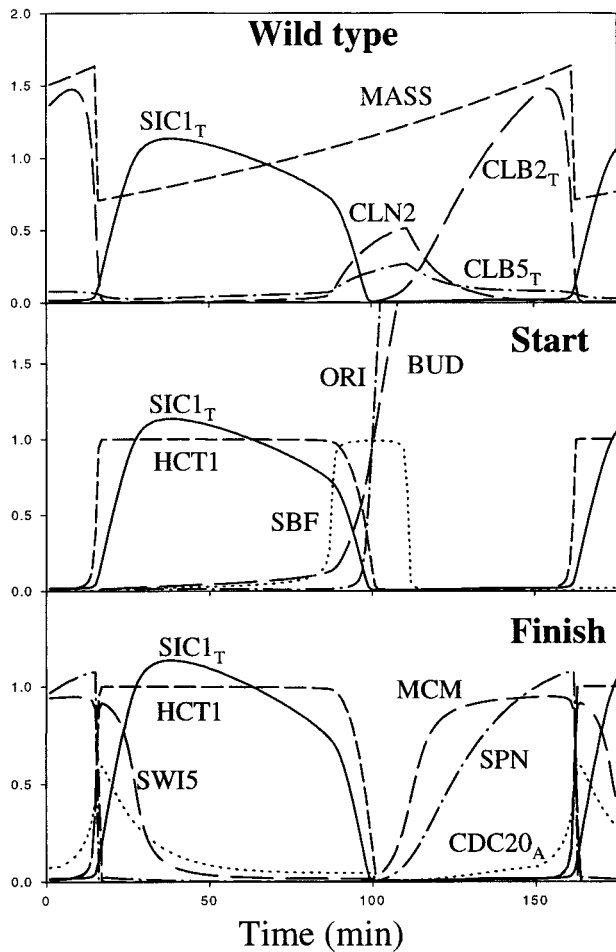
Figure 3. Wild-type cell cycle in daughter cells. Computed from equations and parameter values in Tables 1 and 2.

Under Rule 2, simulations show that mother cells become slightly larger each cycle for the first few cycles (Table 3, line 1) but not as much as the observed 25% increase (Hartwell and Unger, 1977; Johnston *et al.*, 1979); furthermore, mother cells soon reach a steady size. This discrepancy is tied inevitably (in our model) to the prominent unbudded phase of mother cells (Figure 1). Under Rule 2, mother cell birth size is less than the critical mass for SBF activation. Hence, mother cells have an extended unbudded phase, as they grow to this critical mass, and mother cell cycles, like daughter cell cycles, are size regulated. Consequently, mother size at division does not increase steadily with each generation. Under Rule 1, size control is absent from mother cells, and they do grow larger each generation, as observed, but Rule 1 does not fit the observations in Figure 1. We do not know how to resolve this problem.

Similar to the observation of Lord and Wheals (1980), Johnston *et al.* (1977) reported that the smaller a cell is at birth the longer its unbudded interval is. These data support the proposal that smaller cells need more time to grow to a critical size for bud initiation. Our simulations (Figure 4) agree closely with these observations.

Analysis of Mutants

Dependence of Cell Size on CLN3 Gene Dosage. That Cln3 plays a major role in size control of budding yeast is suggested by the strong dependence of mean cell size on *CLN3* gene dosage (Cross, 1988; Nash *et al.*, 1988; Dirick *et al.*, 1995; Yaglom *et al.*, 1995). Figure 5 presents the model's simulation of this effect. The fact that cells approach a minimal size as *CLN3* dosage increases suggests that the activity of Cln3-dependent kinase plateaus at high concentration (assumption 5). The parameter J_{n3} determines how fast $[Cln3]^*$, the kinase activity of Cln3, saturates with increasing *CLN3* dosage, D_{n3}.

Role of the Positive Feedback Loop. Experimental evidence clearly shows that SBF can be activated by Cln1–2 and Clb5–6 as well as Cln3 (Cross and Tinkelenberg, 1991; Schwob and Nasmyth, 1993), hence the appearance of all three CDK activities in $V_{a,sbf}$ (Table 1). In wild-type cells Clb5 can play no role in SBF activation at Start, because any Clb5 present in G1 phase will be tied up in inactive trimers, Sic1/Clb5/Cdc28. However, some active Cln2-dependent kinase is likely present in G1, and it could cooperate with Cln3 and Bck2 in activating SBF. This positive feedback loop (SBF turns on Cln2 synthesis, and Cln2/Cdc28 activates SBF) could potentially play a major role in the activation of SBF at Start.

Dirick *et al.* (1995) and Stuart and Wittenberg (1995) addressed the role of positive feedback by comparing cell size at SBF activation in two mutant strains, *cln1 cln2* and *cln3*. Each strain was made artificially small at birth by ectopic expression of a wild-type *CLN* gene carried on a plasmid. Dirick *et al.* (1995) used *CLN2* under the control of a methionine-repressible promoter. In the presence of methionine (plasmid-borne *CLN2* not expressed), both strains are larger than normal, and SBF is activated soon after cell division. Cell size in this case is not indicative of the minimum size necessary to activate SBF. To assay the minimum size, cells were grown in the absence of methionine (plasmid-borne *CLN2* expressed), so that they grow and divide, like wild type, at a much smaller size. The smallest newborn cells (volume ~10 fl) were selected by centrifugal elutriation and resuspended in medium containing methionine. In this case, the cells needed to grow awhile before SBF was activated. Cells of the *cln1 cln2 MET-CLN2* strain activated SBF at 19 fl, exactly the same size as control cells (*CLN1 CLN2 CLN3 MET-CLN2*). On the other hand, cells lacking Cln3 (the *cln3 MET-CLN2* strain) activated SBF at ~45 fl (Dirick *et al.*, 1995, their Figure 2A).

These remarkable results indicate that 1) positive feedback does not play a determinative role in the activation of SBF at Start (because cell size at SBF activation is unchanged when the positive feedback loop is broken); and 2) there must be some component (other than Cln1–3 and Clb5,6) that turns on SBF in the absence of Cln3, albeit at a larger size. (Clb5,6 are excluded because deletion mutants have size similar to that of wild-type cells, not twice as big.)

To capture these features with our model, we assume that Cln3 is much more efficient than Cln2 in activating SBF ($\varepsilon_{sbf,n3} \gg 1$), and that Cln3 is assisted by Bck2 (reasons to be described later). Because the *cln3* mutant is about twice the size of wild type, we choose parameters so that Bck2 and

Table 3. Properties of wild-type cells and *cln* mutants

	Mass at birth	Mass at SBF 50%	Mass at DNA repl.	Mass at bud ini.	Mass at division	T_{G1} (min)	Changed parameter	Comments (Experimental results in boldface type)
1 wild type (daughter)	0.71	1.07 (71′)	1.15 (84′)	1.15 (84′)	1.64 (146′)	84		CT 146 min (time of occurrence of event)
1st parent	0.93	1.07	1.17	1.16	1.67	39		CT 101 min
2nd parent	0.95	1.08	1.18	1.17	1.68	37		CT 99 min
3rd parent	0.96	1.08	1.18	1.17	1.69	36		CT 98 min
2 *cln3*	1.24	2.04	2.20	2.15	2.88	99	$D_{n3} = 0$	**Dirick, 1995, Fig. 3, size 1.7 × WT**
3 *cln3 sic1*	1.09	1.85	1.28	1.90	2.54	28	$D_{n3} = 0$ $k'_{s,c1} = 0$ $k''_{s,c1} = 0$	G1 short, size 1.5 × WT, smaller than *cln3*
4 *CLN3^D*	0.44	0.45	0.49	0.52	1.02	17	$D_{n3} = 8$	**Yaglom, 1995, protein 8×, size 75% WT Cross, 1988, Fig. 3, Nash, 1988, Fig. 1, size 60% WT**
cln3 GAL-CLN3	0.43	0.43	0.46	0.50	0.99	14	$D_{n3} = 20$	**Tyers, 1992, Table 1, protein 20 × WT, size 44% WT**
5 *cln3 GAL-CLN3 sic1*	0.42	0.42	0.45	0.49	0.98	12	$D_{n3} = 20$ $k'_{s,c1} = 0$ $k''_{s,c1} = 0$	SBF activated early, G1 short, cells small
6 *cln1 cln2*	1.46	1.47	2.47	2.58	3.39	91	$k'_{s,n2} = 0$ $k''_{s,n2} = 0$	**Dirick, 1995, Fig. 3, size 3.2 × WT**
7 *cln1 cln2 sic1*	0.81	1.12	0.97	1.29	1.89	31	$k''_{s,n2} = 0$ $k'_{s,c1} = 0$ $k''_{s,c1} = 0$	**Dirick, 1995, Fig. 4, size between *cln1 cln2* and WT**
8 *cln1 cln2 clb5 clb6*	0.71	1.23	[11.66]	No bud	[14.44]		$k''_{s,n2} = 0$ $k'_{s,b5} = 0$ $k''_{s,b5} = 0$	**Schwob, 1993, Fig. 5, G1 arrest** We consider cells arrested in G1 if mass at DNA replication exceeds 5
9 *cln1 cln2 GAL-CLN2*	0.34	0.34 (1′)	0.38 (23′)	0.35 (6′)	0.78 (146′)	23	$k'_{s,n2} = 0.1$ $k''_{s,n2} = 0$	**Dirick, 1995, Fig. 6, size small, budding is advanced more than DNA replication when compared with WT**
10 *cln1 cln2 GAL-CLN2 sic1*	0.33	0.33	0.36	0.34	0.76	19	$k'_{s,n2} = 0.1$ $k''_{s,n2} = 0$ $k'_{s,c1} = 0$ $k''_{s,c1} = 0$	SBF activated early, G1 short, cells small.
11 *cln1 cln2 MET-CLN2 GAL-SIC1*	0.39	0.39	0.48	0.40	0.90	38	$k'_{s,n2} = 0.1$ $k''_{s,n2} = 0$ $k'_{s,c1} = 0.1$ $k''_{s,c1} = 0$	Birth size between *GAL-CLN2* and *GAL-SIC1* (0.80)
12 *cln1 cln2 MET-CLN2 clb1 clb2 GAL-CLB2*	0.20	No SBF	0.33	0.22	0.47	85	$k'_{s,n2} = 0.1$ $k''_{s,n2} = 0$ $k'_{s,b2} = 0.1$ $k''_{s,b2} = 0$	Steady-state mass at birth = 0.20 (28% WT); cells may not be viable at this size. See Fig. 7

Note: to simulate mutants that synthesize cyclins constitutively, e.g., *cln1 cln2 GAL-CLN2*, we set the rate constant for regulated synthesis to zero ($k''_s = 0$) and the rate constant for unregulated synthesis to a uniform value ($k'_s = 0.1$) to represent a constant rate of expression from the *GAL* promoter. This is a neutral assumption, in the absence of any quantitative data about levels of mRNA expression driven by the *GAL* promoter.

Cln3 contribute about equally to SBF activation. Simulations of the experiments of Dirick *et al.* (1995) are presented in Figure 6, A–C.

In the *cln1 cln2* strain (Figure 6B), the events that normally occur together at Start are dissociated. First, SBF turns on at mass = 1.2 (volume = 24 fl), slightly larger than in wild-type cells (22 fl). (We use the conversion factor 1 mass unit = 20 fl.) Because Cln1 and Cln2 are missing, Sic1 degradation and Hct1 inactivation are delayed. Cells must grow larger (~35 fl) before the combined effects of Cln3 and Clb5 can remove Sic1 (Cln3 phosphorylates and destabilizes Sic1, whereas Clb5 titrates away Sic1). With Sic1 gone, the rapidly rising Clb5-associated kinase activity initiates DNA synthesis, bud emergence, and Hct1 inactivation. Then, as Clb2 appears, cells enter mitosis.

Start events in the *cln3* strain (Figure 6C) occur at even larger size, because these cells rely on Bck2 alone to activate SBF. Once SBF turns on (at ~41 fl), subsequent events of the cell cycle occur normally.

Properties of cln Mutants. When cycling, recessive *cln3* mutant cells are 75% larger than wild-type cells, whereas dominant *CLN3^D* mutant cells are 40% smaller, and double
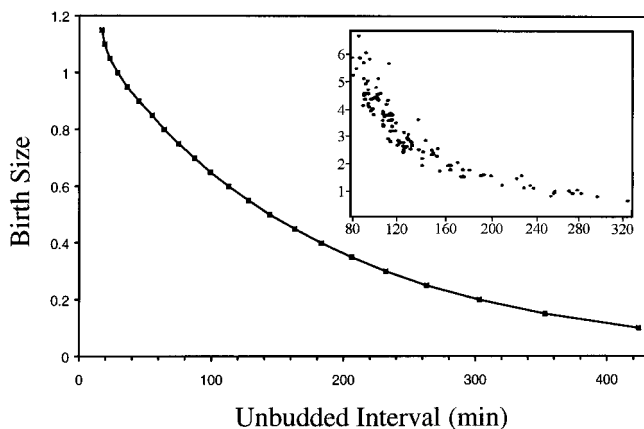
Figure 4. Length of the unbudded interval of daughter cells depends inversely on birth size. Inset, experimental results from Figure 5 of Johnston *et al.* (1977), used by permission.

recessive *cln1 cln2* mutant cells are twice as large, all in agreement with observations (Table 3, lines 2, 4, and 6; Cross, 1988; Nash *et al.*, 1988; Dirick *et al.*, 1995).

In the paper by Dirick *et al.* (1995), the authors reported an intriguing phenomenon. As previously described, *cln1 cln2* mutants, when started very small (10 fl), initiate DNA synthesis and budding at ~40 fl (their Figure 4). However, in cycling *cln1 cln2* cells, DNA synthesis and budding is delayed further to 60 fl (their Figure 3). That is, although the birth size of the cycling cells is ~32 fl, they are unable to initiate DNA synthesis and budding at 40 fl but have to grow larger still (60 fl) to do these jobs. Why?

Our simulation (Figure 6D) gives an explanation. In the cycling culture, when cells reach 40 fl (which occurs soon after birth), there is still abundant Sic1, because Swi5 is active in early G1, and Sic1 degradation is slow in the absence of Cln2. It takes ~1 h to remove Sic1 by a combination of Cln3-dependent phosphorylation of Sic1 and Clb5 binding to Sic1. As soon as $[Clb5]_T \approx [Sic1]_T$, Clb5-depen-
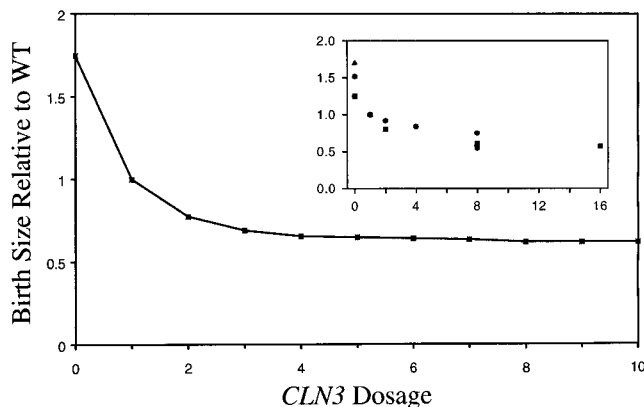
Figure 5. Dependence of cell size on *CLN3* dosage. Inset, experimental results compiled from Cross (1988), Dirick *et al.* (1995), Nash *et al.* (1988), and Yaglom *et al.* (1995).

dent kinase activity starts to rise and initiates DNA synthesis. In our simulation, cycling *cln1 cln2* cells (born at mass = 1.46, 29 fl) begin DNA synthesis at mass = 2.47 (Table 3, line 6, equivalent to 49 fl); whereas for very small cells (born at mass = 0.71, 14 fl), DNA synthesis begins at mass = 1.75, equivalent to 35 fl. These results are in reasonable agreement with the observations of Dirick *et al.* (1995). Without the help of Clb5, as in the case of the *cln1 cln2 clb5 clb6* mutant, Cln3-dependent kinase has a hard time fighting against Sic1 alone, and cells are inviable, blocked in G1 (Table 3, line 8).

When Cln2 is synthesized constitutively (*cln1 cln2 GAL-CLN2*; Table 3, line 9), cells are smaller than normal. Because Cln2-dependent kinase activity is always high, Start occurs shortly after division, and size control at the G1/S transition is lost. Nonetheless, this strain is perfectly viable, and its cell cycle is still size regulated. As pointed out by Futcher (1996), this observation implies a size control mechanism in M phase that is cryptic as long as size control at Start is operating. In our model, this stems largely from the mass dependence of the positive feedback loop that activates Clb2 transcription. In small cells, the rise of Clb2-dependent kinase activity is delayed, which lengthens the duration of M phase. Bypassing transcriptional control of Clb2 can test this explanation: cells constitutively expressing both Cln2 and Clb2 (*cln1 cln2 MET-CLN2 clb1 clb2 GAL-CLB2*) should be considerably smaller than cells constitutively expressing Cln2 alone (*cln1 cln2 MET-CLN2*) (Figure 7 and Table 3, lines 9 and 12). Such small cells may be inviable.

Rescue of Triple-cln Mutant. Especially noteworthy is the inviable *triple-cln* mutant *cln1 cln2 cln3* (Table 4, line 2). SBF is activated by Bck2 (at a larger than normal size), but no other events of Start occur, because they all require CDK activity (the Clns are all missing, and the Clbs are all inhibited by Sic1). In our simulations, the cell eventually grows large enough for the low, G1 level of Clb5 to turn off Hct1 and Sic1 and then to initiate DNA synthesis and progress toward mitosis, but S/M commences at such a large size, 5 times larger than in wild-type, that the cell, we assume, has already died.

Clearly, the *triple-cln* mutant can be rescued by supplying *CLN2* or *CLN3* on a plasmid with a *GAL* promoter (Table 4, lines 3 and 4). It can also be rescued by *GAL-CLB5* (Table 4, line 6) or simply by providing an extra genomic copy of *CLB5* (Table 4, line 6), as observed (Epstein and Cross, 1992). In the latter case, Clb5 is made twice as fast, so cells are able to turn off Sic1 and Hct1 at a reasonable size. In addition, *triple cln* can be rescued by deleting the genomic copy of *SIC1* (Schneider *et al.*, 1996; Tyers, 1996) (see Figure 6F and Table 4, line 8; the mechanism for the rescue will be described later).

However, *triple-cln* mutants cannot be rescued by *GAL-CLB2* (Table 4, line 7); cells remain arrested in G1 because active Hct1/APC keeps Clb2 level low (Amon *et al.*, 1994). Nor can it be rescued by *hct1* or *apc* mutations (Table 4, lines 9 and 10), as observed (Irniger and Nasmyth, 1997; Schwab *et al.*, 1997); here DNA synthesis can be initiated, but cells cannot exit from mitosis (more on this later).

Role of Bck2. Bck2 has not received much attention from molecular biologists, but what is known (Epstein and Cross, 1994; Di Como *et al.*, 1995) is consistent with the role given
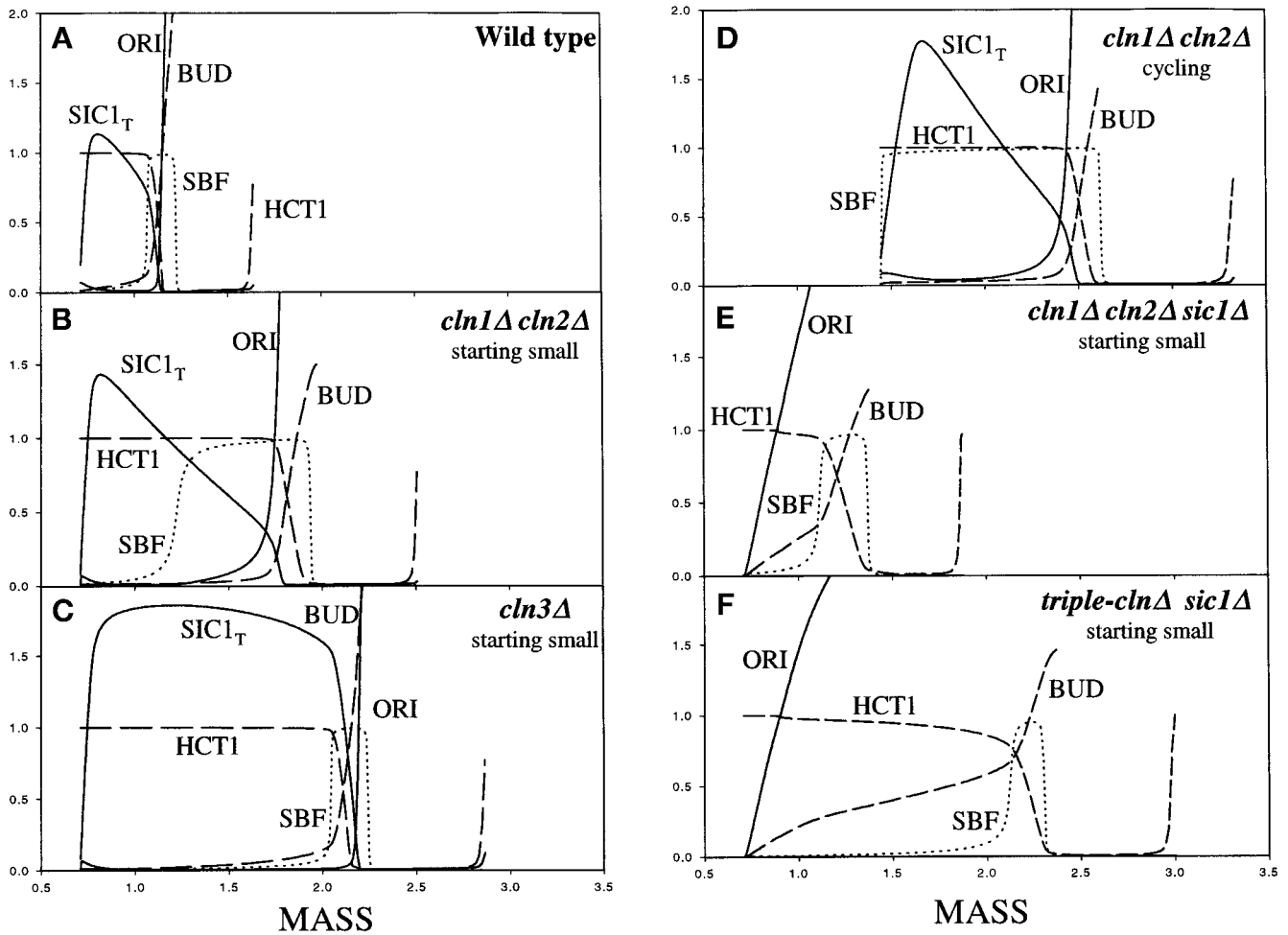
Figure 6. Dissociation of Start events in *cln* mutants. (A–C) Compare with experiments of Dirick *et al.* (1995). (A) In wild-type cells, several molecular and physiological events occur together at Start: activation of SBF, inactivation of Hct1, proteolysis of Sic1, initiation of DNA synthesis, and emergence of a bud. (B) In *cln1Δ cln2Δ* cells, these events are dissociated: SBF is activated at wild-type size, but all other events are delayed until the cell gets much larger. (C) In *cln3Δ* cells, the events are again concurrent, but they occur at about twice the size of wild-type cells. (D) Under steady-state conditions, *cln1Δ cln2Δ* cells are much larger than wild type. SBF is activated immediately. However, DNA synthesis is much delayed (to mass = 2.47), beyond the size at which it would occur (at mass = 1.75) in B. This delay is due to the burst of Sic1 synthesis at anaphase. (E) Deletion of *SIC1* from *cln1Δ cln2Δ* suppresses the delay of bud emergence, as observed by Dirick (1995), and pushes DNA synthesis to a size smaller than in wild-type (contrary to their observation). In the absence of inhibitor, the small level of Clb5 early in the cycle is effective in driving DNA synthesis and bud emergence. See text for further discussion. (F) Deletion of *SIC1* rescues the inviable *cln1Δ cln2Δ cln3Δ* mutant. DNA synthesis begins at a small size (smaller than in wild type, as observed by Schneider *et al.*, 1996), but all other events of Start are displaced to large size.

to Bck2 in the model (assumption 4). As for the case of *CLN3* mutants, cells overexpressing *BCK2* are smaller than normal (66%), and *bck2* loss-of-function mutants are larger than normal (180%) (Table 5, lines 1b and 1c). Although the triple mutant *cln1 cln2 bck2* (line 2b) is viable and a little larger than *cln1 cln2*, the double mutant *cln3 bck2* (line 3b) is inviable: SBF is never activated, and cells arrest in G1. The inviable *cln3 bck2* cell can be rescued, just like the *triple-cln* mutant, by *GAL-CLN2*, *GAL-CLB5*, or *sic1* (lines 4a–4c). However, because SBF is not activated in this case, it takes more copies of genomic *CLB5* (10 copies vs. 2) for its rescue (line 4d). Modest overproduction of Bck2 rescues *triple-cln*

mutants (line 5b), provided both Swi4 and Swi6 are present, suggesting that Bck2 works through SBF.

Regulation of Clb Proteins. Because Start represents the commitment of a budding yeast cell to a new round of DNA synthesis and division, it is important that B-type cyclins (which drive S phase and mitosis in budding yeast) be inoperative before Start occurs. The Clbs are kept out of the picture in G1 by three mechanisms: 1) *CLB* mRNA transcription is repressed, 2) Clb proteolysis by the APC is active, and 3) a Clb-dependent kinase inhibitor, Sic1, is abundant. In this section we explore the interrelations of
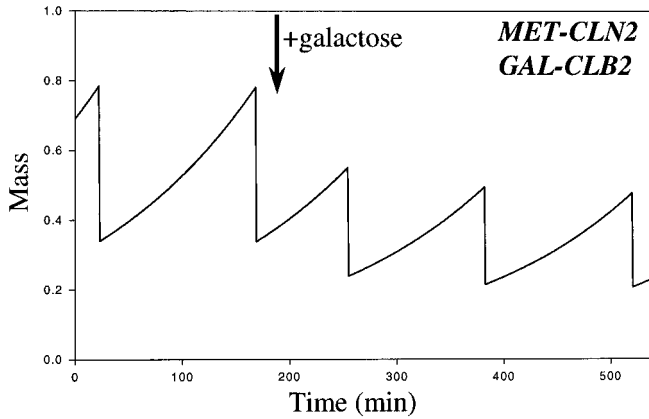
Figure 7. Simulation of *MET-CLN2 GAL-CLB2* (no transcriptional control of Cln2 or Clb2 synthesis). In the absence of both methionine and galactose, cells are smaller than wild type, because Cln2 is synthesized constitutively. When galactose is added (arrow), cells get smaller still, eventually dividing at ~30% of wild-type size. Such small cells may be inviable.

these three effects by simulating mutants that knock out the components singly and in combinations.

First of all, any one of these component processes is expendable. For instance, cells that synthesize Clb2 or Clb5 constitutively (*clb1 clb2 GAL-CLB2* or *clb5 clb6 GAL-CLB5*) are viable (Table 6, lines 3 and 5, and Figure 8, top panel)

(Schwob and Nasmyth, 1993; Surana *et al.*, 1993). *GAL-CLB2* cells are nearly identical to wild-type because active Hct1/APC keeps the Clb2 level low in G1. *GAL-CLB5* cells have abnormally high levels of Clb5 in G1 phase, but abundant Sic1 inhibits the associated CDK activity. Start occurs on schedule when the cell grows large enough for Cln3 + Bck2 to activate SBF, which drives Cln2 accumulation and subsequent phosphorylation (and degradation) of Sic1.

Our model cell can tolerate overexpression of Clb2 better than Clb5. Up to three copies of *GAL-CLB2* are tolerated; four copies or more lead to telophase arrest, as observed (Surana *et al.*, 1993). Abnormally high levels of Clb2 can be tolerated because Clb2 induces its own degradation by stimulating Cdc20 synthesis (Prinz *et al.*, 1998). Higher levels of Cdc20 effectively counteract higher levels of Clb2 at Finish. On the other hand, $2 \times GAL-CLB5$ is lethal because Clb5-associated kinase efficiently phosphorylates and destabilizes Sic1. As a consequence, Sic1 cannot make a comeback at Finish, Clb5/Cdc28 activity stays high, and DNA origins cannot be relicensed in G1.

The *hct1* mutant is also viable (Table 6, line 8, and Figure 8, middle panel) (Schwab *et al.*, 1997). Normally, Clb2 is degraded at the metaphase–anaphase transition, but *hct1* mutants finish the cell cycle differently. At anaphase, Cdc20 activates Swi5 and degrades some Clb2, allowing Sic1 to make a comeback and inhibit any remaining Clb2-dependent kinase activity. Subsequently, Clb2 protein level drops because its transcription turns off.

To model *hct1Δ* mutants correctly, we must assume that Cdc20 accounts for some degradation of Clb2. Three lines of

Table 4. Mutations that rescue the *cln1 cln2 cln3* strain

		Mass at birth	Mass at SBF 50%	Mass at DNA repl.	Mass at bud ini.	Mass at division	T_{G1} (min)	Changed parameter	Comments (Experimental results in boldface type)
1	wild type (daughter)	0.71	1.07 (71')	1.15 (84')	1.15 (84')	1.64 (146')	84		CT 146 min (time of occurrence of event)
2	*cln1 cln2 cln3*	0.71	2.47	[6.20]	[6.48]	[8.11]		$D_{n3}= 0$ $k''_{s,n2}= 0$	**Richardson, 1989, inviable**
3	*cln1 cln2 cln3 GAL-CLN3*	0.65	0.65	0.75	0.95	1.50	25	$D_{n3}= 20$ $k''_{s,n2}= 0$	**Schwob, 1993, Fig. 2, SBF activated soon after galactose induction**
4	*cln1 cln2 cln3 GAL-CLN2*	0.34	0.34	0.39	0.35	0.79	25	$D_{n3}= 0$ $k'_{s,n2}= 0.1$ $k''_{s,n2}= 0$	**Cross, 1991, Fig. 4, *GAL-CLN1* induces *cln2***
5	*cln1 cln2 cln3 2X CLB5*	2.81	2.83	4.96	5.15	6.52	98	$D_{n3}= k''_{s,n2}=0$ $k'_{s,b5}= 0.012$ $k''_{s,b5}= 0.04$	**Epstein, 1992, viable**
6	*cln1 cln2 cln3 GAL-CLB5*	1.23	2.07	2.05	2.14	2.86	88	$D_{n3}= k''_{s,n2}=0$ $k'_{s,b5}= 0.1$ $k''_{s,b5}= 0$	**Schwob, 1993, Fig. 6, viable**
7	*cln1 cln2 cln3 GAL-CLB2*	0.71	2.57	[5.49]	[6.64]	[7.38]		$D_{n3}= k''_{s,n2}=0$ $k'_{s,b2}= 0.1$ $k''_{s,b2}= 0$	**Amon, 1994, Fig. 8, G1 arrest** We consider cells arrested in G1 if mass at DNA replication exceeds 5
8	*cln1 cln2 cln3 sic1*	1.30	2.12 (85')	1.50 (24')	2.24 (94')	3.01 (146')	24	$D_{n3}= k''_{s,n2}=0$ $k'_{s,c1}= 0$ $k''_{s,c1}= 0$	**Tyers, 1996, Fig. 2, viable but large**
9	*cln1 cln2 cln3 hct1*	0.71	2.48	4.62	5.03	No mit		$D_{n3}= k''_{s,n2}=0$ $k''_{d,b2}= 0.01$	**Schwab, 1997, Fig. 3, M phase arrest**
10	*cln1 cln2 cln3 apc-ts*	0.71	2.48	4.16	4.60	No mit		$D_{n3}= k''_{s,n2}=0$ $k''_{d,b2}= 0.01$ $k'''_{d,b2}= 0$ $k'''_{d,b5}= 0$	**Irniger, 1997, Fig. 2, M phase arrest**

Table 5. Properties of *bck2* mutants

Genotype		Cell size relative to wild type			
		Observed			
		Epstein[a]	Di Como[b]	Dirick[c]	Simulation
1a	*CLN1 CLN2 CLN3 BCK2*	1	1	1	1
b	*bck2*	1.3	1.5		1.8
c	+ low-copy *BCK2*		0.8		0.7 with 4 copies
2a	*cln1 cln2 CLN3 BCK2*	1.5		3.2	2.1
b	*bck2*	1.7			2.6
3a	*CLN1 CLN2 cln3 BCK2*	1.7	1.5	1.7	1.7
b	*bck2*	Inviable	Inviable		Inviable
4a	*CLN1 CLN2 cln3 bck2*				
	+ *GAL-CLN2*		Rescued		0.5
b	+ *GAL-CLB5*				1.9
c	+ *sic1*				2.8
d	+ low-copy *CLB5*				3.7 with 10 copies
5a	*cln1 cln2 cln3 BCK2*	Inviable	Inviable		Inviable
b	+ low-copy *BCK2*	Rescued			3.9 with 4 copies

[a] Epstein and Cross (1994).

[b] Di Como *et al.* (1995).

[c] Dirick *et al.* (1995).

evidence support this assumption (10). Experiments of Irniger *et al.* (1995, their Figure 4) show that Clb2 is partially degraded in *cdc15* telophase-arrested cells when (we presume) Cdc20 is active and Hct1 is not. Visintin *et al.* (1997, their Figure 2) showed that Clb2 is degraded by both Hct1 and Cdc20 in nocodazole-arrested cells. Finally, it is well known that sister chromatid separation and B-type cyclin degradation are mediated by a single Cdc20 homologue during early embryogenesis of *Drosophila* and *Xenopus* (Dawson *et al.*, 1995; Sigrist *et al.*, 1995; Lorca *et al.*, 1998).

The ability of Sic1 to bring Hct1-deficient cells out of mitosis depends on cell size: in the presence of α-factor, *hct1* cells grow very large, replicate their DNA, and block in mitosis (Schwab *et al.*, 1997). Our simulation of *cln1 cln2 cln3 hct1* behaves similarly (Table 6, line 9). By the time the mitotic checkpoint is satisfied and cells are ready to divide, they are so big and their accumulated Clb2 level is so high that Sic1 is unable to win over Clb2.

Although *sic1* is sick (having many deficiencies in chromosome dynamics), it is still a viable mutant (Table 6, line 6, and Figure 8, bottom panel). The only major change in the timing of cell cycle events is the advancement of DNA synthesis (relative to bud emergence) by ~35 min (Schneider *et al.*, 1996, their Figure 4). These authors show that *sic1* cells initiate DNA synthesis at a much smaller size than wild-type cells.

Because in wild-type cells DNA synthesis and SBF activation occur almost concurrently, and SBF activation depends mainly on the actions of Cln3 and Bck2 (not inhibited by Sic1), it follows that in *sic1* mutants initiation of DNA synthesis is well ahead of SBF activation. That is, the small amount of Clb5, synthesized by an MBF-independent pathway, is able to initiate DNA synthesis at a small size (because there is no Sic1 present to inhibit it), well before the cell is large enough to activate SBF.

In contrast to the viability of single mutants (*GAL-CLBs*, *hct1*, and *sic1*), double mutants are all inviable (Table 6, lines 9–13). *hct1 sic1* cells, being unable to eliminate Clb2-dependent kinase, cannot exit mitosis (Visintin *et al.*, 1997). *clb5 GAL-CLB5 sic1* cells complete one cycle after adding galactose but die in the second cycle because they cannot replicate their DNA (they cannot resynthesize licensing factor, because Clb-dependent kinase activity stays high after mitosis) (Schwob *et al.*, 1994). *clb2 GAL-CLB2 sic1* cells die after adding galactose, because they cannot bud (SBF is kept off by high Clb2-dependent kinase activity after mitosis). For the same reason, *clb2 GAL-CLB2 hct1* and *clb5 GAL-CLB5 hct1* cells are inviable.

Properties of SIC1^{op} Mutants. Twofold overexpression of Sic1 is tolerated (Verma *et al.*, 1997), but (roughly) 10-fold overexpression is deleterious (Nugroho and Mendenhall, 1994): some 20% of the cells have elongated buds and fail to divide. Our simulations of *sic1 GAL-SIC1* (Table 6, line 7, with $k''_{s,c1} = 0$ and increasing $k'_{s,c1}$ up to fivefold from 0.1 to 0.5) give viable cells with increasing G1 period and larger sizes, but a sixfold increase is lethal (DNA synthesis commences at mass > 5). This behavior is consistent with the experimental observations, provided cells in a population have a distribution of levels of Sic1 production. Similarly, cells with the phosphorylation sites of Sic1 removed (protein stable) never enter S phase (Table 6, line 7), as observed (Verma *et al.*, 1997).

The reason that cells tolerate high levels of Sic1 expression (i.e. 5 × *GAL-SIC1*) and still go through DNA synthesis and mitosis is because of the role played by *CLN2*. SBF activation is unaffected by Sic1; however, high levels of Sic1 inhibit Clb2 activity, so SBF inactivation is delayed. Cln2 will be synthesized at a high rate for longer time, and eventually

Table 6. Properties of *clb, sic1,* and *hct1* mutants

	Mass at birth	Mass at SBF 50%	Mass at DNA repl.	Mass at bud ini.	Mass at division	T_{G1} (min)	Changed parameter	Comments
1 wild type (daughter)	0.71	1.07 (71')	1.15 (84')	1.15 (84')	1.64 (146')	84		CT 146 min (time of occurrence of event)
2 *clb1 clb2*	0.71	1.07	1.16	1.16	No mit		$k'_{s,b2}=0$ $k''_{s,b2}=0$	**Surana, 1991, Table 1, G2 arrest**
3 *clb1 clb2 1X GAL-CLB2*	0.65	1.10	1.19	1.19	1.50	105	$k'_{s,b2}=0.1$	**Surana, 1993, Fig. 4, 1X *GAL-CLB2* is OK, 4X *GAL-CLB2* (or 1X *GAL-CLB2db*) causes telophase arrest**
clb1 clb2 4X GAL-CLB2	0.71	No SBF	1.50	No bud	inviable		$k''_{s,b2}=0$ $k'_{s,b2}=0.4$ $k''_{s,b2}=0$	
clb1 clb2 GAL-CLB2db	0.71	No SBF	0.73	No bud	No mit		$k'_{s,b2}=0.1$ $k''_{s,b2}=0$ $k''_{d,b2}=0.01$ $k'''_{d,b2}=0$	
4 *clb5 clb6*	0.73	1.07 (65')	1.30 (99')	1.17 (80')	1.70 (146')	99	$k'_{s,b5}=0$ $k''_{s,b5}=0$	**Schwob, 1993, Fig. 4, DNA repl. begins 30 min after SBF activation**
5 *clb5 clb6 GAL-CLB5*	0.61	0.93	0.92	0.96	1.41	73	$k'_{s,b5}=0.1$	**Schwob, 1993, Fig. 6, DNA repl. concurrent with SBF activation in both *GAL-CLB5* and *GAL-CLB5db***
clb5 clb6 2X GAL-CLB5	0.71 (1st) 0.57 (2nd)	0.87 0.58	0.87 No repl	0.89 0.58	1.33		$k''_{s,b5}=0$ $k'_{s,b5}=0.2$ $k''_{s,b5}=0$	First cycle OK, but prerepl. complex cannot form after the first cycle and cell dies
clb5 clb6 GAL-CLB5db	0.71 0.65	1.01 0.65	1.02 No repl	1.04 0.66	1.51		$k'_{s,b5}=0.1$ $k''_{s,b5}=0$ $k''_{d,b5}=0$	**Schwob, 1994, Fig. 3, DNA repl. is not advanced in the first cycle**
6 *sic1*	0.66	1.00 (73')	0.82 (37')	1.06 (83')	1.52 (146')	38	$k'_{s,c1}=0$ $k''_{s,c1}=0$	**Schneider, 1996, Fig. 4, *sic1*Δ uncouples S phase from budding**
7 *sic1 GAL-SIC1*	0.80	1.07	1.38	1.17	1.86	94	$k'_{s,c1}=0.1$	**Verma, 1997, Fig. 3B, Nugroho and Mendenhall, 1994, Fig. 2, most cells are viable**
sic1 GAL-SIC1db	0.71	1.07	No repl	1.17	No mit		$k''_{s,c1}=0$ $k'_{s,c1}=0.1$ $k''_{s,c1}=0$ $k_{d2,c1}=0$	**Verma, 1997, Fig. 3, G1 arrest**
8 *hct1*	0.73	1.08	1.17	1.18	1.69	82	$k''_{d,b2}=0.01$	**Schwab, 1997, Fig. 2, viable, size like WT, Clb2 level high throughout the cycle**
9 *hct1*	0.71	No SBF	0.72	No bud	No mit		$k'_{s,c1}=0$ $k''_{s,c1}=0$ $k''_{d,b2}=0.01$	**Visintin, 1997, telophase arrest**
10 *sic1 GAL-CLB5*	0.71 (1st) 0.52 (2nd)	0.74	0.73 No repl	0.76	1.20		$k'_{s,b5}=0.1$ $k''_{s,b5}=k'_{s,c1}=$ $k''_{s,c1}=0$	**Schwob, 1994, Fig. 7C, inviable** First cycle OK, DNA repl. advanced; but prerepl. complexes cannot form and cell dies after the first cycle
11 *hct1 GAL-CLB5*	0.71	No SBF	0.72	0.77	No mit		$k'_{s,b5}=0.1$ $k''_{s,b5}=0$ $k''_{d,b2}=0.01$	
12 *sic1 GAL-CLB2*	0.71	No SBF	0.81	No bud	No mit		$k'_{s,b2}=0.1$ $k''_{s,b2}=k'_{s,c1}=$ $k''_{s,c1}=0$	Cells die in first cycle, no bud
13 *hct1 GAL-CLB2*	0.71	No SBF	0.83	No bud	No mit		$k'_{s,b2}=0.1$ $k''_{s,b2}=0$ $k''_{d,b2}=0.01$	
14 *sic1 clb5 clb6*	0.74	1.08	1.32	1.18	1.72	99	$k'_{s,c1}=k''_{s,c1}=$ $k'_{s,b5}=k''_{s,b5}=0$	Behaves very much like *clb5 clb6*

they will be able to phosphorylate Sic1, causing it to degrade and Clb kinases to win.

Initiation of DNA Synthesis in the sic1 Mutant. As described in the previous section, when compared with wild-type cells, *sic1* mutants initiate S phase at a much smaller size, whereas *cln1 cln2* mutants initiate it at a much larger size (Dirick *et al.*, 1995). What will happen if the two mutations are combined?

Because, in *sic1* mutants, initiation of DNA synthesis is driven mainly by the small amount of Clb5 present in early G1 cells, deletion of Clns should have little effect on its timing. Hence, the multiple mutants *cln1 cln2 sic1* or *cln1 cln2 cln3 sic1* all should initiate DNA synthesis at about the same size as the *sic1* single mutant, at a size smaller than wild type.

Our simulation (Figure 6F) of *cln1 cln2 cln3 sic1* agrees with observations of Schneider *et al.* (1996, their Figure 4B). Without Sic1 inhibition, Clb5 is able to initiate DNA synthesis early and
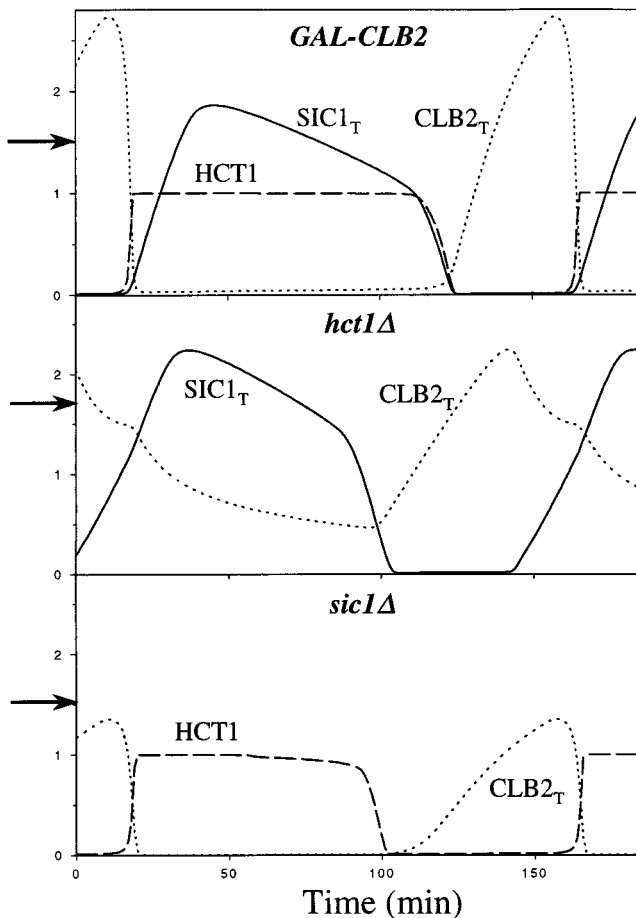
Figure 8. Cells are able to exit from mitosis when any single one of the three Clb2-inhibiting mechanisms is faulty. Top panel, constitutive transcription of *CLB2* in G1 phase. Middle panel, no Hct1-mediated degradation of Clb2 at telophase. Bottom panel, no Sic1 to inhibit Clb2/Cdc28 in G1 phase. The arrow on the ordinate indicates mass at division; all three strains have size comparable with wild type.

to help Bck2 turn on SBF and MBF, causing more Clb5 accumulation, Hct1 inactivation, and eventually progression toward mitosis.

However, for *cln1 cln2 sic1*, the simulation (Figure 6E) does not agree with observations. Dirick *et al.* (1995, their Figure 4) reported that DNA synthesis occurs at about the same size for the mutant as for wild-type cells. If the observation of Schneider *et al.* (1996) is true, then how can the addition of a functional *CLN3* gene (giving *cln1 cln2 sic1*) delay DNA synthesis to a larger mass, when Cln3 is a helper to Clb5? Thus, we are unable to fit all these observations with our present understanding of the control system, and we believe that the experimental observation of Dirick *et al.* (1995) requires closer investigation.

DISCUSSION

In Figure 2, we propose a realistic mechanism for regulating the cell division cycle in budding yeast. Its components are

Cln1 and 2 (lumped together), Cln3 and Bck2, Clb1 and 2 (lumped), Clb5 and 6 (lumped), Sic1, Hct1 (=Cdh1), and Cdc20. (Cdc28, the kinase subunit that combines with the cyclins, is present in excess, so we need not keep track of its fluctuations.) In addition, the model tracks the relative activities of three transcription factors, Swi4/Swi6 (=SBF), Mcm1/SFF, and Swi5, which determine the rates of synthesis of Cln2, Clb2, and Sic1, respectively. At present, we assume that MBF, the transcription factor for Clb5, is regulated coordinately with SBF. In the model, overall cell growth is exponential, and the basic events of the yeast division cycle (DNA synthesis, budding, and spindle assembly) are driven by the integrated activities of cyclin-dependent kinases. These assumptions lead to a mathematical model (Table 1) consisting of 10 nonlinear, ordinary differential equations (for mass, the cyclins, and their consorting proteins), three algebraic functions for transcription factors, three "integrators" to trigger DNA synthesis, budding, and spindle assembly, and a simple rule for separating mother and daughter cells at division.

The kinetic model introduces ~50 parameters (rate constants, binding constants, thresholds, relative efficiencies, etc.) that need to be determined by fitting specific experimental observations. For the present, we do this by trial and error (Appendix A), so we can only claim that our model equations and parameter set are *sufficient* to account for many properties of cell cycle control in budding yeast. Because we fit the model to the properties of dozens of different genotypes, we have enough data to fix the parameters and to provide meaningful confirmation of the mechanism in Figure 2.

Table 2 is in no sense an *optimal* parameter set, nor can we quantify how *robust* is the system, although our experience suggests that the model is quite hardy. Currently we are working on computational methods of parameter optimization and sensitivity analysis and hope to address these problems in a later publication.

Bistability and Hysteresis

The crucial idea behind our model of the budding yeast cell cycle is Nasmyth's (1996) hypothesis that G1 and S/M are alternative, self-maintaining states, generated by mutual antagonism between Clb-dependent kinases and their opponents, Sic1 and Hct1. In theoretical terms, the molecular regulatory system exhibits bistability and hysteresis (Figure 9). In its "neutral" condition (no Cln2 or Cdc20), the control system can persist in either the stable G1 state or the stable S/M state. Transitions between these alternative steady states can be driven by changes in Cln2 and Cdc20 that push the control system past the "fold" points in Figure 9 (Novak *et al.*, 1998).

At Start, Cln2-dependent kinase activity rises abruptly and pushes the cell from G1 to S/M by inactivating Hct1 and promoting Sic1 degradation (Figure 9, stage *a*). The Clns can drive this transition because they are neither degraded by Hct1 nor inhibited by Sic1. After Clb2 appears, Cln2 is removed, but the cell remains in S/M because the Clbs can now keep Hct1 and Sic1 in abeyance without further help from Clns (stage *b*). This effect, called hysteresis, makes the Start transition irreversible.

Cdc20, activated at metaphase, pushes the cell from S/M to G1 (Finish) by activating Hct1 and promoting Sic1 accu-
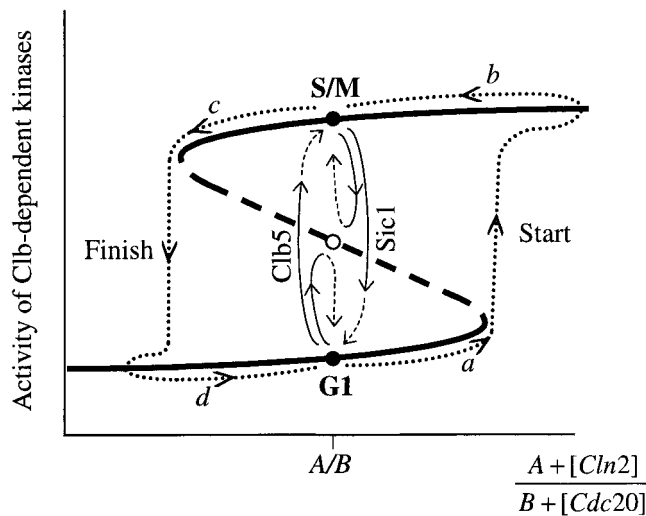
Figure 9. Bistability and hysteresis (schematic). Steady-state level of total Clb-dependent kinase activity depends on the expression of *CLN2* and *CDC20*. When [Cln2] is large and [Cdc20] is small, the Clb–6 regulatory system is in a state of high kinase activity (S/M), whereas in the other extreme, Clb-dependent kinase activity is low (G1). When [Cln2] and [Cdc20] are both small, the regulatory system is in neutral (background activity = *A/B*), and two stable states of Clb activity coexist (bistability). The system is driven around a hysteresis loop (dashed curve) by pulses of Cln2 (stages *a* and *b*) and Cdc20 (stages *c* and *d*).

mulation (Figure 9, stage *c*). Cdc20 can drive this transition, because it is not opposed by Clb-dependent kinase activities; indeed, Clb2 promotes Cdc20 accumulation and activation. As Cdc20 is destroyed in G1 (stage *d*), the control system does not flip back to the S/M state, because Hct1 and Sic1 can now keep the Clbs in abeyance without further help from Cdc20. The S-shaped curve in Figure 9 accounts for the characteristic irreversibility of entry into S phase and exit from mitosis.

In this picture, not merely *may* the "pushers" be removed and the control system will not revert, but they *must* be removed to make a repeated sequence of properly regulated Start and Finish transitions. For instance, once Start is accomplished, Cln2 must disappear; otherwise it will work against the Finish transition. Higher concentrations of Cdc20 will be required to trigger Finish. Furthermore, after the cell leaves mitosis, as Cdc20 disappears, Sic1 and Hct1 will not be able to hold the cell in G1. For these reasons, although *GAL-CLN2* mutants are viable, they have short G1 and long S/M periods.

Similarly, removal of Cdc20 after Finish is crucial for the next Start transition. Because the phosphatase (Cdc14) activated by Cdc20 can overwhelm all CDK activity at metaphase and thereby induce Finish, then it will be difficult to induce the next Start if Cdc20 activity does not disappear in G1 phase so that this phosphatase can be inactivated. In this regard, notice that mild overproduction of Cdc20 (*GAL-CDC20* in 0.2% galactose) induces prolongation of G1 (Prinz *et al.*, 1998), and strong overproduction (3X *GAL-CDC20* in 2% galactose) induces G1 arrest (Shirayama *et al.*, 1998). *GAL-CDC14* also induces G1 arrest (Visintin *et al.*, 1998).

Direct experimental confirmation of bistability can be sought by holding the control system in neutral (Figure 9, position A/B) and then driving it between G1 and S/M by ectopic expression of Clb5 and Sic1 (Figure 9, vertical arrows). This experiment has been done in part by Dahmann *et al.* (1995). After arresting cells in mitosis with nocodazole, they induced transition to G1 (without nuclear or cell division) by ectopic expression of Sic1. When ectopic synthesis of Sic1 was repressed, their cells executed a second round of DNA synthesis, because endogenous production of Clns drove the cells through Start. To prevent autonomous reentry into S phase, we suggest that cells be blocked with α-factor as well as nocodazole.

We propose that a synchronous culture of *MET-CLB5 TET-SIC1* cells (where *MET* = methionine-repressible promoter and *TET* = tetracycline-inducible promoter), about to execute Start and bud, be transferred from "growth" medium (containing methionine) to "arrest" medium (containing methionine, α-factor, and nocodazole). (Notice that the use of α-factor and nocodazole to arrest cells in neutral could be replaced by *cln1–3Δ* and *clb1–4Δ*, respectively.) Those cells that have not yet executed Start when the medium is changed will be kept in G1 phase by α factor (moving from *a* to G1 in Figure 9), whereas those cells that have already executed Start will be arrested in M phase by nocodazole (moving from *b* to S/M in Figure 9). The culture is now a mixed population of G1- and S/M-arrested cells, suggesting that, in this neutral position, there coexist two stable steady states of Clb activity. To prove the coexistence of these states, divide the culture into two batches. One batch is subjected to transient Clb5 synthesis by transferring the cells briefly to "Clb5" medium (α-factor + nocodazole) and then back to arrest medium. All cells in this batch are expected to arrest in the S/M state (in Figure 9, cells initially at G1 will be driven to S/M, whereas those initially at S/M will return there). Cells of the other batch, after brief exposure to "Sic1" medium (methionine + tetracycline + α-factor + nocodazole), are expected to arrest uniformly in G1 phase. Furthermore, the duration of the "brief" exposure is important: there should be threshold levels of exposure to Clb5 and Sic1 below which the transitions are not accomplished (see Figure 9).

Note that, at the end of treatment, all cells are of uniform size and are exposed to arrest medium. Nonetheless, if our model is correct, individual cells will be in different phases of the division cycle, depending on how they were perturbed. Those cells initially in G1 will be pushed into S/M by a Clb5 perturbation but not by a Sic1 perturbation (Schwob and Nasmyth, 1993) and vice versa for those cells initially in S/M (Dahmann *et al.*, 1995). This behavior would indicate that two stable states of Clb activity coexist (bistability) when the regulatory system is in neutral. By alternating treatment with Clb5 and Sic1, one should be able to induce multiple rounds of endoreplication in *cln1–3Δ clb1–4Δ* cells.

Reversibility of the SBF Switch

In contrast to the irreversibility of the Start and Finish transitions, the activation of SBF in our model is a reversible, ultrasensitive switch. To test this feature of the model, one could modify slightly the experimental design of Dirick *et al.* (1995). The strain *cln1Δ cln2Δ cln3^ts MET-CLN2* is grown in

the absence of methionine, so that newborn daughter cells are small. Small cells, transferred to methionine-containing medium at permissive temperature, will activate SBF (measured by expression of *PCL1* mRNA, say) at wild-type size, but Sic1 degradation and Hct1 activation will be delayed to a much larger size. If, after SBF activation, the cells are transferred to restrictive temperature, then SBF should inactivate (i.e., this event is reversible), and the cells should remain in G1.

Autonomously Oscillating Versus Checkpoint-controlled Cell Cycles

Cell division cycles of budding yeast (and somatic cells in general) are blocked by drugs that inhibit DNA replication or spindle assembly ("checkpoint controls"), whereas early embryonic cell divisions are unrestrained by these same drugs (Murray and Hunt, 1993). If somatic and embryonic cells use the same cell cycle control machinery, why do they behave so differently?

In theoretical terms, checkpoints correspond to stable steady states (G1 and S/M in the current model), and drugs that inhibit growth, DNA synthesis, or spindle assembly abort the signals that normally push the cell from one checkpoint to the next. The existence of these checkpoints depends on the mutual antagonism between cyclin B-dependent kinases and their opponents (Sic1 and Hct1 homologues).

In early *Xenopus* embryos, there are no effective antagonists of cyclin B/Cdc2 kinase (also called MPF). 1) The only identified MPF inhibitors are p28[Kix1] (Shou and Dunphy, 1996) and p27[Xic1] (Su *et al.*, 1995), but both are present at very low levels until the late gastrula stage. Furthermore, neither one inhibits MPF in vitro. 2) *XFZR* (the *Xenopus* homologue of *HCT1*) is not translated before the midblastula transition. Instead, X-FZY (the *Xenopus* homologue of Cdc20) is responsible for cyclin B degradation during early embryonic cell cycles (Lorca *et al.*, 1998). X-FZY, like Cdc20, seems to be activated rather than inhibited by MPF (Felix *et al.*, 1990). 3) Even the antagonistic relationship between MPF and Wee1 (a tyrosine kinase that inhibits Cdc2) seems to be ineffective, because Cdc2 shows very little tyrosine 15 phosphorylation during the early cycles of intact embryos (Ferrell *et al.*, 1991).

Without effective antagonists in early embryonic cells, MPF cannot establish the alternative steady states characteristic of checkpoint controls. The only remaining control is a time-delayed negative feedback loop, whereby MPF activates X-FZY, which degrades cyclin B and thereby destroys MPF activity. The sufficiency of this mechanism to generate autonomous oscillations in MPF activity was shown first by Goldbeter (1991) and later by Novak and Tyson (1993). Because the early embryo lacks cyclin B antagonists, it supports rapid MPF oscillations that are insensitive to errors in DNA replication and spindle assembly; apparently the early embryo has sacrificed accuracy for speed. However, in frog egg extracts, checkpoint control can be elicited if a sufficient amount of unreplicated sperm DNA is added (Dasso and Newport, 1990; Smythe and Newport, 1992), which creates an effective antagonist by activating Wee1. If our hypothesis is right, one may be able to elicit checkpoint responses in *Xenopus* embryos before the midblastula transition by injecting *XFZR* mRNA (or protein) into the fertilized egg.

Models as Tools in Molecular Biology

Undoubtedly the genetic regulatory system of cell division in yeast and higher eukaryotes is even more complex than Figure 2. To understand regulatory systems of such complexity, we need analytical tools that can handle realistic biochemical control mechanisms. Our work confirms that modern methods of kinetic theory and computation are capable of connecting a realistic, multilayered, regulatory mechanism to the complex physiological behavior of cells.

In addition to its role in synthesizing molecular and physiological details about cell division, the model is a predictive tool. The rate constant estimates in Table 2 can be tested by more direct kinetic measurements. Tables 3–6 specify many quantitative properties of mutant cells that have never been reported, and they predict phenotypes of several mutants yet to be examined.

One can learn as much from the failures of the model as from its successes. Where there are inconsistencies between the model and experiment, we are prompted, first of all, to look for a better parameter set. If that fails, we consider slight changes in the mechanism, which might bring the model in accord with observations. If that fails, and if the experimental community is convinced that the observations are reliable and significant, then we have identified an area that deserves closer scrutiny to resolve the discrepancies. If the mechanism proves insufficient, that does not invalidate our approach. Mathematical modeling, as a tool, is no more "falsifiable" than gel electrophoresis. The tool tells us what a mechanism can and cannot explain. When the model fails, the fault lies with the mechanism, not the tool.

The molecular mechanism of cell cycle control in budding yeast is an evolving hypothesis that must be continually examined, revised, and improved as new observations tell us more about the control system. We intend to extend the model in several directions. First, we will provide a more detailed description of Finish (Novak *et al.*, 1999), including roles for Cdc14 (Visintin *et al.*, 1998; Jaspersen *et al.*, 1999), RENT complexes (Shou *et al.*, 1999), and Pds1/Esp1 interactions (Ciosk *et al.*, 1998; Cohen-Fix and Koshland, 1999; Tinker-Kulberg and Morgan, 1999). The next step will be to connect mathematical representations of surveillance mechanisms to the underlying cell cycle engine. For instance, the mating factor pathway connects pheromone binding at the cell surface, through a protein kinase cascade, to the inhibition of Cln kinases, which arrests cells before Start (Wittenberg and Reed, 1996; Posas *et al.*, 1998). Another important signal transduction pathway, through *mad* and *bub* gene products, arrests cells in mitosis, if the mitotic spindle is improperly assembled (Alexandru *et al.*, 1999; Taylor, 1999).

APPENDIX A: ESTIMATION OF RATE CONSTANTS

First some definitions:

1) A Michaelis constant (J in our notation) carries units of concentration (nM). In the Michaelis–Menten rate law, J is the characteristic substrate concentration at which reaction rate is half-maximal.

2) A zero-order rate constant carries units of nM min^{-1}. Examples include rates of synthesis (k_s in our notation), and V_{max} values in Michaelis–Menten rate laws (k_a and k_i in our notation).

3) A first-order rate constant carries units of min^{-1}. Examples include degradation rate constants (k_d) and dissociation rate constants (k_{di}).

4) A second-order rate constant, e.g., an association rate constant (k_{as}), carries units of nM^{-1} min^{-1}.

In writing the kinetic equations in Table 1, all concentration variables are scaled so that their maximal values are pure numbers of order 1. We are forced to do this because little is known about the actual concentrations (nM) of any of the molecular components in budding yeast cells. Because all concentration variables are dimensionless, the Michaelis constants are dimensionless, and all the zero-, first-, and second-order rate constants carry units of min^{-1} (Table 2).

Rates of Degradation

Because the stability of cyclins at various stages in the budding yeast cell cycle has been studied carefully by many experimental groups, we can estimate the cyclin degradation constants in our model with some confidence. For instance, the half-life Cln2 is 5–10 min (Salama *et al.*, 1994; Barral *et al.*, 1995; Lanker *et al.*, 1996), implying that $k_{d,n2} \approx \ln2/7 = 0.1$ min^{-1}, which is the value we use (Table 2). Because Hct1 is turned off at Start, Clb2 is more stable in S/M than in G1: half-life = 1 min in G1 and > 1 h in S/M (Amon *et al.*, 1994; Irniger *et al.*, 1995; Seufert *et al.*, 1995). These observations imply that $k'_{d,b2} \approx \ln2/70 = 0.01$ min^{-1} and $k''_{d,b2} \approx \ln2/1 = 0.7$ min^{-1}, which are close to the values in Table 2. Clb5, on the other hand, is only slightly more stable in S/M (half-life = 10 min) than in G1 (half-life = 2 min) (Irniger and Nasmyth, 1997). Hence, $k'_{d,b5} \approx \ln2/10 = 0.07$ min^{-1}, and $k'_{d,b5} + k''_{d,b5} \approx \ln2/2 = 0.35$ min^{-1} (see Table 2).

From the observed half-life of Cdc20, 15 min (Shirayama *et al.*, 1998), we estimate that $k_{d,20} = 0.05$ min^{-1}.

Sic1 disappears at Start over the course of ~20 min (Schwob *et al.*, 1994). Because we use a Michaelis–Menten rate law for Sic1 phosphorylation (the rate-limiting step for Sic1 degradation at Start), it is not so obvious how to estimate our rate parameters, but the values $J_{d2,c1} \ll 1$ and $k_{d2,c1} = 0.3$ min^{-1} give reasonable agreement to Schwob's observation.

Rates of Synthesis

Rate constants for cyclin synthesis can be estimated from degradation rate constants and steady-state concentrations. However, because the concentrations are unknown, we cannot ascribe directly meaningful values to the synthesis rate constants. Instead, we choose $k_s \approx k_d$, so that the maximum concentrations of all variables during a wild-type cycle are ~1. The chosen values of k_s reflect the relative concentrations of the cyclins, Sic1, and Cdc20, as best we can guess, but the arbitrary units (au) in which each concentration is expressed are unknown until we have better experimental data. For instance, suppose the peak concentrations of Sic1 and Cln2 were measured to be 100 and 30 nM, respectively. Then, from Figure 3, we would assign 1 au of Sic1 concentration = 90 nM and 1 au of Cln2 concentration = 60 nM, and we could predict that $k'_{s,c1} = 1.8$ nM min^{-1}, $k''_{s,c1} = 9$ nM min^{-1} (when Swi5 is fully active), $J_{d2,c1} = 4.5$ nM, and $k_{d2,c1} = 0.3$ min^{-1} (90/60 nM) = 0.45 min^{-1}.

Rates of Association and Dissociation

The rate constant (k_{as}) for association of Sic1 with Clb2/Cdc28 and Clb5/Cdc28 is an important parameter in the model. It must be large enough to account for strong binding, given reasonable lability of the complexes ($k_{di} = 0.05$ min^{-1}, assumed). We choose $k_{as} = 50$ min^{-1}, which implies a binding constant of 10^3. The theory of diffusion-controlled reactions (Tinoco *et al.*, 1978, p. 385) puts an upper limit on second-order rate constants: $k_{max} = 8\pi r N_o D_{avg}$, where r = encounter distance of a pair of reacting molecules, N_o = Avogadro's number, and D_{avg} = average diffusion coefficient of the reacting molecules. Assuming r = 4×10^{-7} cm, and $D_{avg} = 2 \times 10^{-6}$ cm^2 s^{-1}, we estimate that $k_{max} = 10^{10}$ l mol^{-1} s^{-1} = 10 nM^{-1} s^{-1}. If the concentration of protein partners is roughly 80 nM, then k_{max} (scaled) $\approx 5 \times 10^4$ min^{-1}, which is 1000 times larger than the value assigned to k_{as}.

Rates of Activation and Inactivation

The transcription factors SBF, Mcm1, and Swi5 are each described by Goldbeter–Koshland functions, $G(V_a, V_i, J_a, J_i)$. (Please refer to Appendix B for the definition of this function and a detailed description of its properties.) When J_a and J_i are much less than 1, a Goldbeter–Koshland function changes very abruptly in the neighborhood of G = ½. Because the SBF switch turns on abruptly as cells grow (Dirick *et al.*, 1995), we choose $J_{a,sbf}$ and $J_{i,sbf}$ to be small (0.01). By contrast, we suppose that Mcm1 turns on and off more smoothly ($J_{a,mcm} = J_{i,mcm} = 1$).

Activation and inactivation of Hct1 is also governed by a Goldbeter–Koshland mechanism, but we do not make a pseudo–steady-state approximation (d[Hct1]/dt = 0). Rather,

$$\frac{d}{dt}[Hct1] = \frac{(k'_{a,t1} + k''_{a,t1}[Cdc20]) \cdot ([Hct1]_T - [Hct1])}{J_{a,t1} + [Hct1]_T - [Hct1]}$$
$$- \frac{\{k'_{i,t1} + k''_{i,t1}([Cln3]^* + \varepsilon_{i,t1,n2}[Cln2] + \varepsilon_{i,t1,b5}[Clb5] + \varepsilon_{i,t1,b2}[Clb2])\}[Hct1]}{J_{i,t1} + [Hct1]}$$

The rates at which Hct1 switches between more and less active forms depend on the rate constants, k_a and k_i. We expect they have values of order 1 min^{-1}, so that changes occur in minutes rather than seconds or hours. More precise estimates cannot be made from presently available measurements.

To estimate the conditions for turning Hct1 on and off, we notice that [Hct1] $\approx$ ½[Hct1]$_T$ when

$$k'_{a,t1} + k''_{a,t1}[Cdc20] = k'_{i,t1} + k''_{i,t1}([Cln3]^* + \varepsilon_{i,t1,n2}[Cln2]$$
$$+ \varepsilon_{i,t1,b5}[Clb5] + \varepsilon_{i,t1,b2}[Clb2])$$

(provided $J_{a,t1} = J_{i,t1}$). In metaphase, when Clb2 plays the major role in keeping Hct1 inactive, the condition for activating Hct1 is [Cdc20] = $k''_{i,t1}$[Clb2]/$k''_{a,t1} \approx 0.5$. That is, Hct1 turns on when Cdc20 activity exceeds 0.32 × Clb2 activity. The threshold can be adjusted by changing the ratio $k''_{i,t1}/k''_{a,t1}$. In late G1 phase, when [Cdc20] ≈ 0.05, [Clb2] $\approx$ 0, [Cln3]$^* \ll$ [Cln2], and Clb5 is still inhibited by Sic1, the condition for inactivating Hct1 is [Cln2] = $(k'_{a,t1} + k''_{a,t1}[Cdc20])/k''_{i,t1} \approx 0.2$. With our choice of parameters, Cln2 plays the major role in turning off Hct1 at Start. It may be that Clb5 plays a more important role, in which case the

relative efficiencies ($\varepsilon_{i,t1,b5}$ and $\varepsilon_{i,t1,n2}$) would have to be readjusted.

Other Parameters

$[Cln3]_{max} = 0.02$ is chosen so that the amount of Cln3 at Start, $[Cln3]^* \approx 0.003$ when mass ≈ 1, is ~100 times smaller than the maximum amounts of Cln1 and Cln2 during the cycle (Tyers *et al.*, 1993). Although Cln3 is present in a very small amount, it plays an important role turning on SBF at Start (Dirick *et al.*, 1995; Stuart and Wittenberg, 1995), because $\varepsilon_{sbf,n3}$ is very large. $[Bck2]^0 = 0.0027$ is chosen to account for the observed size for SBF activation in the *cln3* mutant.

Efficiencies

Our model contains many other dimensionless "efficiencies" of different CDKs for various phosphorylation reactions. These efficiencies simply represent the fact that budding yeast cyclins have overlapping specificities: they often catalyze the same reactions but with different relative turnover numbers. We adjusted the efficiencies to account for the relative timing of events in mutants where the primary cyclin is missing and the event is triggered by one of its backups.

For instance, in *triple-clnΔ sic1Δ*, Clb5 is the primary cyclin responsible for Hct1 inactivation. If $\varepsilon_{i,t1,b5}$ were too small, then Hct1 would never turn off, and the mutant would be inviable. If $\varepsilon_{i,t1,b5}$ were too large, then the small amount of uninhibited Clb5 early in the cycle (which drives premature DNA synthesis in this mutant) would inactivate Hct1 too soon. As a result, Clb2 would rise early, and SBF could never be activated, so the mutant would divide at a small size without ever making a bud. In our simulations, $\varepsilon_{i,t1,b5} \approx 0.5$ gives a correct phenotype to this mutant.

Integrators

Finally, we have introduced three "integrators" (ORI, BUD, and SPN), which determine when the events of 1) initiation of DNA synthesis, 2) bud emergence, and 3) chromosome alignment on the mitotic spindle will occur. Experiments show that 1) DNA synthesis can be initiated by Clbs but not by Clns (Schwob *et al.*, 1994); 2) bud emergence can be driven by Clb5 as well as Clns (Schwob and Nasmyth, 1993), and 3) mitosis can be driven to completion only by Clb1 and Clb2 (Surana *et al.*, 1991). These facts determine the forms taken by the integrators. The rate constants ($k_{s,ori}$, $k_{s,bud}$, and $k_{s,spn}$) and efficiencies are chosen to give the right timing of these events in various mutants.

Note that some parameters are introduced only for notational consistency (e.g., $k_{a,sbf}$, $k_{a,mcm}$, $k_{a,swi}$, and $k_{i,t1}$) and are set equal to 1 or 0 in all computations. Other parameters are constrained to be identical (e.g., $J_{a, ...} = J_{i, ...}$), to limit the scope of the problem. Therefore, we had ~50 parameters to estimate from the properties of ~50 different genotypes. Wild-type cells provide us with enough information to estimate more than half of these parameters. The remaining parameters are constrained by the properties of all the mutants we have simulated. Because each viable mutant gives us at least two pieces of information (relative size and G1 duration), we have much more data to fit than parameters to

vary. Therefore, because the model accounts for so many facts (in quantitative detail wherever possible), we conclude that the molecular mechanism in Figure 2 is essentially correct.

APPENDIX B: ZERO-ORDER ULTRASENSITIVITY

We model the kinetic behavior of the budding yeast transcription factors (SBF, Mcm1, and Swi5) as zero-order ultrasensitive switches (Goldbeter and Koshland, 1981; Ferrell, 1996). We assume that each transcription factor (TF) exists as either an active or inactive form (let F = fraction in active form), and that transitions between the two forms are enzyme-catalyzed reactions following Michaelis–Menten kinetics,

$$\frac{dF}{dt} = \frac{V_a(1-F)}{J_a + 1 - F} - \frac{V_iF}{J_i + F}$$

V_a and V_i are V_{max} values of the activating and inhibiting enzymes, and J_a and J_i are Michaelis constants (relative to the total concentrations of TF). If the transitions are fast enough (V_a and V_i large enough) to keep each TF in its steady-state distribution, then

$$F = G(V_a, V_i, J_a, J_i) = \frac{2\gamma}{\beta + \sqrt{\beta^2 - 4\alpha\gamma}}$$

where $\alpha = V_i - V_a$, $\beta = V_i - V_a + V_aJ_i + V_iJ_a$, and $\gamma = V_aJ_i$. Notice that $G = \frac{1}{2}$ when $V_a/V_i = (2J_a+1)/(2J_i+1)$. If J_a and J_i are both $\ll 1$, then 50% of the TF is active when $V_a/V_i = 1$. Moreover, Goldbeter and Koshland (1981) showed that G is a sharply sigmoidal function of V_a/V_i if J_a and J_i are $\ll 1$.

In our model, this behavior shows up as a sharp activation of SBF by Cln3-dependent kinase, as the cell grows through a critical size. To calculate the size at which $[SBF] = \frac{1}{2}$, we set $V_a = V_i$,

$$k_{a,sbf}\{[Cln2] + \varepsilon_{sbf,n3}([Cln3]^* + [Bck2]) + \varepsilon_{sbf,b5}[Clb5]\} = k'_{i,sbf} + k''_{i,sbf}[Clb2]$$

Noting that $[Cln2] \approx [Clb5] \approx [Clb2] \approx 0$ in G1, we find that $[SBF] = \frac{1}{2}$ when

$$k_{a,sbf} \cdot \varepsilon_{sbf,n3}\left([Cln3]_{max}\frac{D_{n3} \cdot mass}{J_{n3} + D_{n3} \cdot mass} + [Bck2]^0 \cdot mass\right) = k'_{i,sbf}$$

or, given the parameter values listed in Table 2,

$$\frac{3 \cdot mass}{6 + mass} + 0.4 \cdot mass = 1$$

The solution of this quadratic equation is mass ≈ 1.2. This is the critical size for SBF activation; in wild-type cells, all other events of Start occur in rapid succession after the cell activates SBF. (In the full model, SBF activates at a slightly smaller size, presumably because of the residual activities of the other kinases in G1, which we neglected in this calculation.)

REFERENCES

Alberts, B., Bray, D., Lewis, J., Raff, M., Roberts, K., and Watson, J.D. (1994). Molecular Biology of the Cell, 3rd ed., New York: Garland Publishing.

Alexandru, G., Zachariae, W., Schleiffer, A., and Nasmyth, K. (1999). Sister chromatid separation and chromosome reduplication are regulated by different mechanisms in response to spindle damage. EMBO J. *18*, 2707–2721.

Amon, A. (1997). Regulation of B-type cyclin proteolysis by Cdc28-associated kinases in budding yeast. EMBO J. *16*, 2693–2702.

Amon, A. (1999). The spindle checkpoint. Curr. Opin. Genet. Dev. *9*, 69–75.

Amon, A., Irniger, S., and Nasmyth, K. (1994). Closing the cell cycle circle in yeast: G2 cyclin proteolysis initiated at mitosis persists until the activation of G1 cyclins in the next cycle. Cell *77*, 1037–1050.

Amon, A., Surana, U., Muroff, I., and Nasmyth, K. (1992). Regulation of p34^{CDC28} tyrosine phosphorylation is not required for entry into mitosis in *S. cerevisiae*. Nature *355*, 368–371.

Amon, A., Tyers, M., Futcher, B., and Nasmyth, K. (1993). Mechanisms that help the yeast cell cycle clock tick: G2 cyclins transcriptionally activate G2 cyclins and repress G1 cyclins. Cell *74*, 993–1007.

Bai, C., Sen, P., Hofmann, K., Ma, L., Goebl, M., Harper, J.W., and Elledge, S.J. (1996). Skp1 connects cell cycle regulators to the ubiquitin proteolysis machinery through a novel motif, the F-box. Cell *86*, 263–274.

Baroni, M.D., Monti, P., and Alberghina, L. (1994). Repression of growth-regulated G1 cyclin expression by cyclic AMP in budding yeast. Nature *371*, 339–342.

Barral, Y., Jentsch, S., and Mann, C. (1995). G1 cyclin turnover and nutrient uptake are controlled by a common pathway in yeast. Genes Dev. *9*, 399–409.

Biggins, S., and Murray, A.W. (1998). Sister chromatid cohesion in mitosis. Curr. Opin. Cell Biol. *10*, 769–775.

Botchan, M. (1996). Coordinating DNA replication with cell division: current status of the licensing concept. Proc. Natl. Acad. Sci. USA *93*, 9997–10000.

Carter, B.L.A. (1981). The control of cell division in *Saccharomyces cerevisiae*. In: The Cell Cycle, ed. P.C.L. John, Cambridge, UK: Cambridge University Press, 99–117.

Chang, F., and Herskowitz, I. (1990). Identification of a gene necessary for cell cycle arrest by a negative growth factor of yeast: Far1 is an inhibitor of G1 cyclin, CLN2. Cell *63*, 999–1011.

Cho, R.J., *et al.* (1998). A genome-wide transcriptional analysis of the mitotic cell cycle. Mol. Cell *2*, 65–73.

Ciosk, R., Zachariae, W., Michaelis, C., Shevchenko, A., Mann, M., and Nasmyth, K. (1998). An Esp1/Pds1 complex regulates loss of sister chromatid cohesion at the metaphase to anaphase transition in yeast. Cell *93*, 1067–1076.

Cohen-Fix, O., and Koshland, D. (1999). Pds1p of budding yeast has dual roles: inhibition of anaphase initiation and regulation of mitotic exit. Genes Dev. *13*, 1950–1959.

Cross, F.R. (1988). *DAF*1, a mutant gene affecting size control, pheromone arrest, and cell cycle kinetics of *Saccharomyces cerevisiae*. Mol. Cell. Biol. *8*, 4675–4684.

Cross, F.R., and Tinkelenberg, A.H. (1991). A potential positive feedback loop controlling *CLN1* and *CLN2* gene expression at the start of the yeast cell cycle. Cell *65*, 875–883.

Dahmann, C., Diffley, J.F.X., and Nasmyth, K. (1995). S-phase-promoting cyclin-dependent kinases prevent rereplication by inhibiting the transition of replication origins to a prereplicative state. Curr. Biol. *5*, 1257–1269.

Dasso, M., and Newport, J.W. (1990). Completion of DNA replication is monitored by a feedback system that controls the initiation of mitosis in vitro: studies in *Xenopus*. Cell *61*, 811–823.

Dawson, I.A., Roth, S., and Artavanis-Tsakonas, S. (1995). The *Drosophila* cell cycle gene *fizzy* is required for normal degradation of cyclins A and B during mitosis and has homology to the *CDC20* gene of *Saccharomyces cerevisiae*. J. Cell Biol. *129*, 725–737.

Descombes, P., and Nigg, E.A. (1998). The polo-like kinase Plx1 is required for M phase exit and destruction of mitotic regulators in *Xenopus* egg extracts. EMBO J. *17*, 1328–1335.

Deshaies, R., Chau, V., and Kirschner, M. (1995). Ubiquitination of the G1 cyclin Cln2p by a Cdc34-dependent pathway. EMBO J. *14*, 303–312.

Di Como, C.J., Chang, H., and Arndt, K.T. (1995). Activation of *CLN1* and *CLN2* G1 cyclin gene expression by BCK2. Mol. Cell. Biol. *15*, 1835–1846.

Dirick, L., Bohm, T., and Nasmyth, K. (1995). Roles and regulation of Cln/Cdc28 kinases at the start of the cell cycle of *Saccharomyces cerevisiae*. EMBO J. *14*, 4803–4813.

Donovan, J.D., Toyn, J.H., Johnson, A.L., and Johnston, L.H. (1994). p40^{SDB25}, a putative Cdk inhibitor, has a role in M/G1 transition in *Saccharomyces cerevisiae*. Genes Dev. *8*, 1640–1653.

Epstein, C.B., and Cross, F.R. (1992). *CLB5*: a novel B cyclin from budding yeast with a role in S phase. Genes Dev. *6*, 1695–1706.

Epstein, C.B., and Cross, F.R. (1994). Genes that can bypass the *CLN* requirement for *Saccharomyces cerevisiae* cell cycle START. Mol. Cell. Biol. *14*, 2041–2047.

Feldman, R.M.R., Correll, C.C., Kaplan, K., and Deshaies, R.J. (1997). A complex of Cdc4p, Skp1p and Cdc53/Cullin catalyzes ubiquitination of the phosphorylated CDK inhibitor Sic1p. Cell *91*, 221–230.

Felix, M.-A., Labbe, J.-C., Doree, M., Hunt, T., and Karsenti, E. (1990). Triggering of cyclin degradation in interphase extracts of amphibian eggs by cdc2 kinase. Nature *346*, 379–382.

Ferrell, J.E., Jr. (1996). Tripping the switch fantastic: how a protein kinase cascade can convert graded inputs into switch-like outputs. Trends Biochem. Sci. *21*, 460–466.

Ferrell, J.E., Jr., Wu, M., Gerhart, J.C., and Martin, G.S. (1991). Cell cycle tyrosine phosphorylation of p34^{cdc2} and a microtubule-associated protein kinase homolog in *Xenopus* oocytes and eggs. Mol. Cell. Biol. *11*, 1965–1971.

Futcher, B. (1996). Cyclins and the wiring of the yeast cell cycle. Yeast *12*, 1635–1646.

Goldbeter, A. (1991). A minimal cascade model for the mitotic oscillator involving cyclin and cdc2 kinase. Proc. Natl. Acad. Sci. USA *88*, 9107–9111.

Goldbeter, A., and Koshland, D.E., Jr. (1981). An amplified sensitivity arising from covalent modification in biological systems. Proc. Natl. Acad. Sci. USA *78*, 6840–6844.

Hartwell, L.H., and Unger, M.W. (1977). Unequal division in *Saccharomyces cerevisiae* and its implications for the control of cell division. J. Cell Biol. *75*, 422–435.

Hwang, L.H., Lau, L.F., Smith, D.L., Mistrot, C.A., Hardwick, K.G., Hwang, E.S., Amon, A., and Murray, A.W. (1998). Budding yeast Cdc20: a target of the spindle checkpoint. Science *279*, 1041–1044.

Irniger, S., and Nasmyth, K. (1997). The anaphase-promoting complex is required in G1 arrested yeast cells to inhibit B-type cyclin accumulation and to prevent uncontrolled entry into S-phase. J. Cell Sci. *110*, 1523–1531.

Irniger, S., Piatti, S., Michaelis, C., and Nasmyth, K. (1995). Genes involved in sister chromatid separation are needed for B-type cyclin proteolysis in budding yeast. Cell *81*, 269–277.

Jackson, P.K. (1996). Cell cycle: cull and destroy. Curr. Biol. *6*, 1209–1212.

Jaspersen, S.L., Charles, J.F., and Morgan, D.O. (1999). Inhibitory phosphorylation of the APC regulator Hct1 is controlled by the kinase Cdc28 and the phosphatase Cdc14. Curr. Biol. *11*, 227–236.

Johnston, G.C., Ehrhardt, C.W., Lorincz, A., and Carter, B.L.A. (1979). Regulation of cell size in the yeast *Saccharomyces cerevisiae*. J. Bacteriol. *137*, 1–5.

Johnston, G.C., Pringle, J.R., and Hartwell, L.H. (1977). Coordination of growth with cell division in the yeast *Saccharomyces cerevisiae*. Exp. Cell Res. *105*, 79–98.

King, R.W., Deshaies, R.J., Peters, J.-M., and Kirschner, M.W. (1996). How proteolysis drives the cell cycle. Science *274*, 1652–1659.

Knapp, D., Bhoite, L., Stillman, D.J., and Nasmyth, K. (1996). The transcription factor Swi5 regulates expression of the cyclin kinase inhibitor p40Sic1. Mol. Cell. Biol. *16*, 5701–5707.

Koch, C., Moll, T., Neuberg, M., Ahorn, H., and Nasmyth, K. (1993). A role for the transcription factors Mbp1 and Swi4 in progression from G1 to S phase. Science *261*, 1551–1557.

Koch, C., and Nasmyth, K. (1994). Cell cycle regulated transcription in yeast. Curr. Opin. Cell Biol. *6*, 451–459.

Koch, C., Schleiffer, A., Ammerer, G., and Nasmyth, K. (1996). Switching transcription on and off during the yeast cell cycle: Cln/Cdc28 kinases activate bound transcription factor SBF (Swi4/Swi6) at Start, whereas Clb/Cdc28 kinases displace it from the promoter in G2. Genes Dev. *9*, 129–141.

Kotani, S., Tugendreich, S., Fujii, M., Jorgensen, P.-M., Watanabe, N., Hoog, C., Hieter, P., and Todokoro, K. (1998). PKA and MPF-activated Polo-like kinase regulate anaphase-promoting complex activity and mitosis progression. Mol. Cell *1*, 371–380.

Krek, W. (1998). Proteolysis and the G1-S transition: the SCF connection. Curr. Opin. Genet. Dev. *8*, 36–42.

Lahav-Baratz, S., Sudakin, V., Ruderman, J.V., and Hershko, A. (1995). Reversible phosphorylation controls the activity of cyclosome-associated cyclin-ubiquitin ligase. Proc. Natl. Acad. Sci. USA *92*, 9303–9307.

Lanker, S., Valdivieso, M.H., and Wittenberg, C. (1996). Rapid degradation of the G1 cyclin Cln2 induced by CDK-dependent phosphorylation. Science *271*, 1597–1601.

Leatherwood, J. (1998). Emerging mechanisms of eukaryotic DNA replication initiation. Curr. Opin. Cell Biol. *10*, 742–748.

Li, F.N., and Johnston, M. (1997). Grr1 of *Saccharomyces cerevisiae* is connected to the ubiquitin proteolysis machinery through Skp1: coupling glucose sensing to gene expression and the cell cycle. EMBO J. *16*, 5629–5638.

Lim, H.H., Goh, P.-Y., and Surana, U. (1998). Cdc20 is essential for the cyclosome-mediated proteolysis of both Pds1 and Clb2 during M phase in budding yeast. Curr. Biol. *8*, 231–234.

Lorca, T., Castro, A., Martinez, A.M., Vigneron, S., Morin, N., Sigrist, S., Lehner, C., Doree, M., and Labbe, J.C. (1998). *Fizzy* is required for activation of the APC/cyclosome in *Xenopus* egg extract. EMBO J. *17*, 3565–3575.

Lord, P.G., and Wheals, A.E. (1980). Asymmetrical division of *Saccharomyces cerevisiae*. J. Bacteriol. *142*, 808–818.

Maher, M., Cong, F., Kindelberger, D., Nasmyth, K., and Dalton, S. (1995). Cell cycle-regulated transcription of *CLB2* gene is dependent on Mcm1 and a ternary complex factor. Mol. Cell. Biol. *15*, 3129–3137.

Mendenhall, M.D., and Hodge, A.E. (1998). Regulation of Cdc28 cyclin-dependent protein kinase activity during the cell cycle of the yeast *Saccharomyces cerevisiae*. Microbiol. Mol. Biol. Rev. *62*, 1191–1243.

Murray, A., and Hunt, T. (1993). The Cell Cycle: An Introduction, New York: W.H. Freeman.

Nash, R., Tokiwa, G., Anand, S., Erickson, K., and Futcher, A.B. (1988). The WHI1$^+$ gene of *Saccharomyces cerevisiae* tethers cell division to cell size and is a cyclin homolog. EMBO J. *7*, 4335–4346.

Nasmyth, K. (1993). Control of the yeast cell cycle by Cdc28 protein kinase. Curr. Opin. Cell Biol. *5*, 166–179.

Nasmyth, K. (1995). Evolution of the cell cycle. Philos. Trans. R. Soc. Lond. B *349*, 271–281.

Nasmyth, K. (1996). At the heart of the budding yeast cell cycle. Trends Genet. *12*, 405–412.

Nasmyth, K. (1999). Separating sister chromatids. Trends Biochem. Sci. *24*, 98–104.

Nasmyth, K., Adolf, G., Lydall, D., and Seddon, A. (1990). The identification of a second cell cycle control on the *HO* promotor in yeast: cell cycle regulator of SWI5 nuclear entry. Cell *62*, 631–647.

Nasmyth, K., and Dirick, L. (1991). The role of *SWI*4 and *SWI*6 in the activity of G1 cyclins in yeast. Cell *66*, 995–1013.

Novak, B., Csikasz-Nagy, A., Gyorffy, B., Nasmyth, K., and Tyson, J.J. (1998). Model scenarios for evolution of the eukaryotic cell cycle. Philos. Trans. R. Soc. Lond. B *353*, 2063–2076.

Novak, B., Toth, A., Csikasz-Nagy, A., Gyorffy, B., Tyson, J.J., and Nasmyth, K. (1999). Finishing the cell cycle. J. Theor. Biol. *199*, 223–233.

Novak, B., and Tyson, J.J. (1993). Numerical analysis of a comprehensive model of M-phase control in *Xenopus* oocyte extracts and intact embryos. J. Cell Sci. *106*, 1153–1168.

Novak, B., and Tyson, J.J. (1995). Quantitative analysis of a molecular model of mitotic control in fission yeast. J. Theor. Biol. *173*, 283–305.

Novak, B., and Tyson, J.J. (1997). Modeling the control of DNA replication in fission yeast. Proc. Natl. Acad. Sci. USA *94*, 9147–9152.

Nugroho, T.T., and Mendenhall, M.D. (1994). An inhibitor of yeast cyclin-dependent protein kinase plays an important role in ensuring the genomic integrity of daughter cells. Mol. Cell. Biol. *14*, 3320–3328.

Peter, M., and Herskowitz, I. (1994). Direct inhibition of the yeast cyclin-dependent kinase Cdc28-Cln by Far1. Science *265*, 1228–1231.

Peters, J.-M. (1998). SCF and APC: the yin and yang of cell cycle regulated proteolysis. Curr. Opin. Cell Biol. *10*, 759–768.

Peters, J.-M., King, R.W., Hoog, C., and Kirschner, M.W. (1996). Identification of BimE as a subunit of the anaphase-promoting complex. Science *274*, 1199–1201.

Polymenis, M., and Schmidt, E.V. (1997). Coupling of cell division to cell growth by translational control of the G1 cyclin CLN3 in yeast. Genes Dev. *11*, 2522–2531.

Polymenis, M., and Schmidt, E.V. (1999). Coordination of cell growth with cell division. Curr. Opin. Genet. Dev. *9*, 76–80.

Posas, F., Takekawa, M., and Saito, H. (1998). Signal transduction by MAP kinase cascade in budding yeast. Curr. Opin. Microbiol. *1*, 175–182.

Prinz, S., Hwang, E.S., Visintin, R., and Amon, A. (1998). The regulation of Cdc20 proteolysis reveals a role for the APC components Cdc23 and Cdc27 during S phase and early mitosis. Curr. Biol. *8*, 750–760.

Richardson, H., Lew, D.J., Henze, M., Sugimoto, K., and Reed, S.I. (1992). Cyclin-B homologs in *Saccharomyces cerevisiae* function in S phase and in G2. Genes Dev. *6*, 2021–2034.

Richardson, H.E., Wittenberg, C., Cross, F., and Reed, S.I. (1989). An essential G1 function for cyclin-like proteins in yeast. Cell *59*, 1127–1133.

Salama, S.R., Hendricks, K.B., and Thorner, J. (1994). G1 cyclin degradation: the PEST motif of yeast Cln2 is necessary, but not sufficient, for rapid protein turnover. Mol. Cell. Biol. *14*, 7953–7966.

Schneider, B.L., Yang, Q.-H., and Futcher, B. (1996). Linkage of replication to Start by the Cdk inhibitor Sic1. Science *272*, 560–562.

Schwab, M., Lutum, A.S., and Seufert, W. (1997). Yeast Hct1 is a regulator of Clb2 cyclin proteolysis. Cell *90*, 683–693.

Schwob, E., Bohm, T., Mendenhall, M.D., and Nasmyth, K. (1994). The B-type cyclin kinase inhibitor p40sic1 controls the G1 to S transition in *S. cerevisiae.* Cell *79*, 233–244.

Schwob, E., and Nasmyth, K. (1993). *CLB5* and *CLB6*, a new pair of B cyclins involved in DNA replication in *Saccharomyces cerevisiae*. Genes Dev. *7*, 1160–1175.

Seufert, W., Futcher, B., and Jentsch, S. (1995). Role of a ubiquitin-conjugating enzyme in degradation of S- and M-phase cyclins. Nature *373*, 78–81.

Shirayama, M., Zachariae, W., Ciosk, R., and Nasmyth, K. (1998). The Polo-like kinase Cdc5p and the WD-repeat protein Cdc20p/fizzy are regulators and substrates of the anaphase promoting complex in *Saccharomyces cerevisiae*. EMBO J. *17*, 1336–1349.

Shou, W., and Dunphy, W.G. (1996). Cell cycle control by *Xenopus* p28Kix1, a developmentally regulated inhibitor of cyclin-dependent kinases. Mol. Biol. Cell *7*, 457–469.

Shou, W., Seol, J.H., Shevchenko, A., Baskerville, C., Moazed, D., Chen, Z.W.S., Jang, J., Shevchenko, A., Charbonneau, H., and Deshaies, R.J. (1999). Exit from mitosis is triggered by Tem1-dependent release of the protein phosphatase Cdc14 from nucleolar RENT complex. Cell *97*, 233–244.

Sigrist, S., Jacobs, H., Stratmann, R., and Lehner, C.F. (1995). Exit from mitosis is regulated by *Drosophila fizzy* and the sequential destruction of cyclins A, B, and B3. EMBO J. *14*, 4827–4838.

Skowyra, D., Craig, K.L., Tyers, M., Elledge, S.J., and Harper, J.W. (1997). F-box proteins are receptors that recurit phosphorylated substrates to the SCF ubiquitin-ligase complex. Cell *91*, 209–219.

Smythe, C., and Newport, J.W. (1992). Coupling of mitosis to the completion of S phase in *Xenopus* occurs via modulation of the tyrosine kinase that phosphorylates p34cdc2. Cell *68*, 787–797.

Sorger, P.K., and Murray, A.W. (1992). S-phase feedback control in budding yeast independent of tyrosine phosphorylation of p34cdc28. Nature *355*, 365–368.

Spellman, P.T., Sherlock, G., Zhang, M.Q., Iyer, V.R., Anders, K., Eisen, M.B., Brown, P.O., Botstein, D., and Futcher, B. (1998). Comprehensive identification of cell cycle-regulated genes of the yeast *Saccharomyces cerevisiae* by microarray hybridization. Mol. Biol. Cell *9*, 3273–3297.

Stuart, D., and Wittenberg, C. (1995). *CLN3*, not positive feedback, determines the timing of *CLN2* transcription in cycling cells. Genes Dev. *9*, 2780–2794.

Su, J.-Y., Rempel, R.E., Erikson, E., and Maller, J.L. (1995). Cloning and characterization of the *Xenopus* cyclin-dependent kinase inhibitor p27Xic1. Proc. Natl. Acad. Sci. USA *92*, 10187–10191.

Sudakin, V., Ganoth, D., Dahan, A., Heller, H., Hershko, J., Luca, F.C., Ruderman, J.V., and Hershko, A. (1995). The cyclosome, a large complex containing cyclin-selective ubiquitin ligase activity, targets cyclins for destruction at the end of mitosis. Mol. Biol. Cell *6*, 185–197.

Surana, U., Amon, A., Dowzer, C., McGrew, J., Byers, B., and Nasmyth, K. (1993). Destruction of the CDC28/CLB mitotic kinase is not required for the metaphase to anaphase transition in budding yeast. EMBO J. *12*, 1969–1978.

Surana, U., Robitsch, H., Price, C., Schuster, T., Fitch, I., Futcher, A.B., and Nasmyth, K. (1991). The role of CDC28 and cyclins during mitosis in the budding yeast *S. cerevisiae*. Cell *65*, 145–161.

Taylor, S.S. (1999). Chromosome segregation: dual control ensures fidelity. Curr. Biol. *9*, R562–R564.

Tinker-Kulberg, R.L., and Morgan, D.O. (1999). Pds1 and Esp1 control both anaphase and mitotic exit in normal cells and after DNA damage. Genes Dev. *13*, 1936–1949.

Tinoco, I., Jr., Sauer, K., and Wang, J.C. (1978). Physical Chemistry. Principles and Applications in Biological Sciences, 3rd ed., Upper Saddle River, NJ: Prentice Hall.

Tokiwa, G., Tyers, M., Volpe, T., and Futcher, B. (1994). Inhibition of G1 cyclin activity by the Ras/cAMP pathway in yeast. Nature *371*, 342–345.

Tyers, M. (1996). The cyclin-dependent kinase inhibitor p40sic1 imposes the requirement for Cln G1 cyclin function at Start. Proc. Natl. Acad. Sci. USA *93*, 7772–7776.

Tyers, M., Tokiwa, G., and Futcher, B. (1993). Comparison of the *Saccharomyces cerevisae* G1 cyclins: Cln3 may be an upstream activator of Cln1, Cln2 and other cyclins. EMBO J. *12*, 1955–1968.

Tyson, J.J., Chen, K.C., and Novak, B. (1997). The eukaryotic cell cycle: molecules, mechanisms and mathematical models. In: Case Studies in Mathematical Modeling: Ecology, Physiology and Cell Biology, ed. H.G. Othmer, F.R. Adler, M.A. Lewis, and J.C. Dallon, Upper Saddle River, NJ: Prentice Hall, 127–147.

Tyson, J.J., Novak, B., Chen, K.C., and Val, J. (1995). Checkpoints in the cell cycle from a modeler's perspective. In: Progress in Cell Cycle Research, ed. L. Meijer, S. Guidet, and H.Y.L. Tung, New York: Plenum Press, 1–8.

Tyson, J.J., Novak, B., Odell, G.M., Chen, K., and Thron, C.D. (1996). Chemical kinetic theory as a tool for understanding the regulation of M-phase promoting factor in the cell cycle. Trends Biochem. Sci. *21*, 89–96.

Verma, R., Annan, R.S., Huddleston, M.J., Carr, S.A., Reynard, G., and Deshaies, R.J. (1997). Phosphorylation of Sic1p by G1 Cdk required for its degradation and entry into S phase. Science *278*, 455–460.

Visintin, R., Craig, K., Hwang, E.S., Prinz, S., Tyers, M., and Amon, A. (1998). The phosphatase Cdc14 triggers mitotic exit by reversal of Cdk-dependent phosphorylation. Mol. Cell *2*, 709–718.

Visintin, R., Hwang, E.S., and Amon, A. (1999). Cfi1 prevents premature exit from mitosis by anchoring Cdc14 phosphatase in the nucleolus. Nature *398*, 818–823.

Visintin, R., Prinz, S., and Amon, A. (1997). *CDC20* and *CDH1*: a family of substrate-specific activators of APC-dependent proteolysis. Science *278*, 460–463.

Willems, A.R., Lanker, S., Patton, E.E., Craig, K.L., Nason, T.F., Mathias, N., Kobayashi, R., Wittenberg, C., and Tyers, M. (1996).

Cdc53 targets phosphorylated G1 cyclins for degradation by the ubiquitin proteolytic pathway. Cell *86*, 453–463.

Wittenberg, C., and Reed, S.I. (1996). Plugging it in: signaling circuits and the yeast cell cycle. Curr. Opin. Cell Biol. *6*, 223–230.

Wittenberg, C., Sugimoto, K., and Reed, S.I. (1990). G1-specific cyclins of *S. cerevisiae*: cell cycle periodicity, regulation by mating pheromone, and association with p34CDC28 protein kinase. Cell *62*, 225–237.

Wuarin, J., and Nurse, P. (1996). Regulating S phase: CDKs, licensing and proteolysis. Cell *85*, 785–787.

Yaglom, J., Linskens, H.K., Rubin, D.M., Futcher, B., and Finley, D. (1995). p34Cdc28-mediated control of Cln3 cyclin degradation. Mol. Cell. Biol. *15*, 731–741.

Yamamoto, A., Guacci, V., and Koshland, D. (1996). Pds1p, an inhibitor of anaphase in budding yeast, plays a critical role in the APC and checkpoint pathway(s). J. Cell Biol. *133*, 99–110.

Zachariae, W., and Nasmyth, K. (1999). Whose end is destruction: cell division and the anaphase-promoting complex. Genes Dev. *13*, 2039–2058.

Zachariae, W., Schwab, M., Nasmyth, K., and Seufert, W. (1998). Control of cyclin ubiquitination by CDK-regulated binding of Hct1 to the anaphase promoting complex. Science *282*, 1721–1724.

Zachariae, W., Shin, T.H., Galova, M., Obermaier, B., and Nasmyth, K. (1996). Identification of subunits of the anaphase-promoting complex of *Saccharomyces cerevisiae*. Science *274*, 1201–1204.